AAPG Bulletin

Petroleum generation timing and source in the Northern Longmen Shan Thrust Belt, Southwest China: Implications for multiple oil generation episodes and sources

--Manuscript Draft--

Manuscript Number:	BLTN17-125
Full Title:	Petroleum generation timing and source in the Northern Longmen Shan Thrust Belt, Southwest China: Implications for multiple oil generation episodes and sources
Article Type:	Article
Keywords:	Re-Os geochronology Organic Geochemistry Petroleum evolution Northern Longmen Shan Thrust Belt
Corresponding Author:	Chuanbo Shen China university of Geosciences, Wuhan Wuhan, Hubei CHINA
Corresponding Author Secondary Information:	
Corresponding Author's Institution:	China university of Geosciences, Wuhan
Corresponding Author's Secondary Institution:	
First Author:	Xiang Ge
First Author Secondary Information:	
Order of Authors:	Xiang Ge
	Chuanbo Shen
	David Selby
	Jie Wang
	Liangbang Ma
	Xiaoyan Ruan
	Shouzhi Hu
	Lianfu Mei
Order of Authors Secondary Information:	
Manuscript Region of Origin:	CHINA
Abstract:	The temporal evolution of hydrocarbons (~500 million barrels oil) and its relationship to the orogenic events of the Longmen Shan Thrust Belt have been extensively debated. The hydrocarbons occur as solid bitumen, as dykes and/or coatings within/along faults/fractures, and as present day oil seeps. Here utilizing organic geochemistry, we demonstrate that all the bitumen exhibit similar organo-gechemical characteristics, and were sourced from the Late Neoproterozoic-Early Cambrian Doushantuo and Qiongzhusi formations. In contrast, the organic geochemistry of the present day oil seeps are distinct from that of the bitumen, and suggest that the source is the Permain Dalong Formation. Bitumen rhenium-osmium data indicate that the Late Neoproterozoic-Early Cambrian Doushantuo and Qiongzhusi formations underwent two temporally distinct oil generation events; initially during the Early Ordovician (ca.486 Ma) prior to the Caledonian Orogeny, and secondly during the Jurassic (ca.165 Ma) coinciding with the Indosinian-Yanshan orogenies. In contrast, the rhenium-osmium data of the present day oil seeps are too similar to yield a meaningful age, although the source is considered to have underwent hydrocarbon maturation between the Triassic and Jurassic. The temporal hydrocarbon evolution in the the Longmen Shan Thrust Belt

	also provides implication for the hydrocarbon evolution and future exploration of the adjacent petroliferous Sichuan Basin.
Suggested Reviewers:	Huaning Qiu qiuhn@gig.ac.cn
	Bruce Schaefer Bruce.Schaefer@mq.edu.au
	Naveen Hakhoo naveen@jugaa.com
	Svetoslav Georgiev georgiev@colostate.edu
	Simon Kelley simon.kelley@open.ac.uk
Opposed Reviewers:	Holly Stein holly.stein@colostate.edu We ask that given the publication history between the Colorado State Group and that we are working on very similar topics that this paper is not reviewed by this research group (from Colorado State)
Additional Information:	
Question	**Response**

This is a revised version with the manuscript Number BLTN16-230

Petroleum generation timing and source in the Northern Longmen Shan Thrust Belt, Southwest China: Implications for multiple oil generation episodes and sources

Xiang Ge[1, 2], Chuanbo Shen[1*], David Selby[1, 2], Jie Wang[3], Liangbang Ma[3], Xiaoyan Ruan[1], Shouzhi Hu[1], Lianfu Mei[1]

[1]Key Laboratory of Tectonics and Petroleum Resources (China University of Geosciences), Ministry of Education, Wuhan, 430074, China

[2]Department of Earth Sciences, Durham University, Durham, DH1 3LE, UK

[3]Wuxi institute of petroleum geology, SINOPEC, Wuxi, 214151, China

***Corresponding author E-mail: cugshen@126.com**

Acknowledgement

This work was supported by the National Natural Science Foundation of China (No. 41372140, 41672140, 40902038) and the Fundamental Research Fund for the Central Universities, China University of Geosciences (Wuhan, No. 201536), 111 project (No. B14031)，the Outstanding Youth Funding of Natural Science Foundation of Hubei Province (No. 2016CFA055), the Wuhan Science and Technology Project (No. 2016070204010145), the PetroChina Innovation Foundation (No. 2016D-5007-0103) and a China Scholarship Council (CSC) postgraduate award to Xiang Ge. Selby acknowledges the TOTAL Endowment Fund. We thank Barry J. Katz, Naveen Hakhoo,

Svetoslav Georgiev, Professor Liu, and Rachael Bullock for their constructive comments.

Abstract

The temporal evolution of hydrocarbons (~500 million barrels oil) and its relationship to the orogenic events of the Longmen Shan Thrust Belt have been extensively debated. The hydrocarbons occur as solid bitumen, as dykes and/or coatings within/along faults/fractures, and as present day oil seeps. Here utilizing organic geochemistry, we demonstrate that all the bitumen exhibit similar organo-gechemical characteristics, and were sourced from the Late Neoproterozoic–Early Cambrian Doushantuo and Qiongzhusi formations. In contrast, the organic geochemistry of the present day oil seeps are distinct from that of the bitumen, and suggest that the source is the Permain Dalong Formation.

Bitumen rhenium-osmium data indicate that the Late Neoproterozoic–Early Cambrian Doushantuo and Qiongzhusi formations underwent two temporally distinct oil generation events; initially during the Early Ordovician (ca.486 Ma) prior to the Caledonian Orogeny, and secondly during the Jurassic (ca.165 Ma) coinciding with the Indosinian-Yanshan orogenies. In contrast, the rhenium-osmium data of the present day oil seeps are too similar to yield a meaningful age, although the source is considered to have underwent hydrocarbon maturation between the Triassic and Jurassic. The temporal hydrocarbon evolution in the the Longmen Shan Thrust Belt also provides implication for the hydrocarbon evolution and future exploration of the adjacent petroliferous Sichuan Basin.

1. Introduction

Source rock burial and maturation history, coupled with hydrocarbon generation and subsequent migration are key factors of a petroleum system, which are often temporally

51 associated with regional tectonic events (Bordenave and Hegre, 2005; Moretti et al.,
52 1996; Urien et al., 1995; Yahi et al., 2001). For example, (1) in the Berkine (Ghadames)
53 Basin, eastern Algeria, hydrocarbon maturation of the Silurian, Llandoverian –
54 Wenlockian souce rock and associated oil generation directly relates to the timing of the
55 Cretaceous Austrian Orogeny (Yahi et al., 2001), and (2) in the foreland of the Sub
56 Andean Zone in Bolivia, three stages of tectonic accretion are suggested to have
57 controlled three phases of sedimentation and oil generation during the Cenozoic
58 (Moretti et al., 1996; Urien et al., 1995).
59 The key to understanding the direct relationship between tectonism and the evolution of
60 a petroleum system are the accurate estimates for the timing of the related tectonism and
61 that of the hydrocarbon generation, expulsion and accumulation. Recent successes in
62 determining age constraints and the relationship between tectonism and petroleum
63 evolution has been achieved through the application of both radiometric (e.g., Re-Os,
64 Ar-Ar, Apatite Fission Track (AFT)) and indirect techniques (e.g., basin/tectonic
65 models) (Boles et al., 2004; Fall et al., 2015; Ge et al., 2016).
66 The Sichuan Basin in the South China Block records multiple tectonic events (e.g.,
67 Ordovician-Devonian Caledonian, Late Triassic Indosinian, Late Jurassic Yanshan, and
68 the Cenozoic Himalaya orogenies) (Chen and Wilson, 1996; Dai et al., 2009;
69 Harrowfield and Wilson, 2005; Jin et al., 2010; Sun, 2011; Yan et al., 2011). The
70 majority of the hydrocarbon reserves of the Sichuan Basin are distributed close to its
71 border regions (e.g., Longmen Shan Thrust belt, Micang Shan Uplift, Daba Shan
72 Orogenies) (Li et al., 2015; Li et al., 2001; Liu et al., 2011; Ma et al., 2010) (Fig. 1B).
73 The basin has current reserve estimates of ~30 Bbbl (billions of barrels) of oil and ~180
74 Tcf (Trillion cubic feet) of gas (Zhang and Zhu, 2006; Zou et al., 2014a). Key examples

75 are the giant Puguang Gas field that is located adjacent to the Daba Shan orogenic belt
76 in the northeast Sichuan Basin which possesses ~12 proven original in-place Tcf gas
77 (Ma et al., 2007b), the great Yuanba gas field (~2 Tcf proven gas) that lies near the
78 Micang Shan Uplift in the northern Sichuan Basin (Liu et al., 2011), and several gas
79 fields possessing ~1 Tcf gas (e.g., Dayi, Majing and Pingluoba) that occur near the
80 Longmen Shan Thrust belt (Liu et al., 2011) (Fig. 1B). In addition to the gas fields in
81 the Longmen Shan Thrust belt, hydrocarbons are present as bitumen. The total bitumen
82 accumulation, which is recoverable is estimated to yield a reserve in excess of 500
83 million barrels (Mbbl) of oil (Liu et al., 2003).
84 The Longmen Shan Thrust belt is located between the Songpan-Ganze Terrane and the
85 Sichuan Foreland Basin, and marks the western margin of the Sichuan Basin (Fig. 1A).
86 The belt is tectonically complex due to multiple orogenic events from the Palaeozoic to
87 present (Caledonian, Indosinian–Yanshan, Himalaya) (Jin et al., 2010; Yan et al., 2003).
88 Abundant hydrocarbons predominantly occur in Neoproterozoic to Permian strata and
89 are typically spatially associated with thrust faults and associated fracture systems (Fig.
90 1C) (Dai et al., 2009; Huang and Wang, 2008; Liu et al., 2003). To date, the origin, age
91 and the evolution of the hydrocarbons is debated. For example, either organic-rich strata
92 of the Late Neoproterozoic-Early Cambrian (Dai et al., 2009; Liu et al., 2009; Tian,
93 2009; Wei et al., 2008; Xie et al., 2003) or Permian (Liu et al., 2003; Rao et al., 2008;
94 Wang et al., 1997) are considered to be the main source rocks. Additionally, basin burial
95 history and fluid inclusion analyses propose multiple hydrocarbon generation and
96 migration events, e.g., between the Ordovician and Silurian (Wang and Li, 1999; Wei et
97 al., 2008) and during the Late Triassic (Liu et al., 2009), as well as during the Cenozoic
98 (Liu et al., 2003; Rao et al., 2008).

As a petroleum component, bitumen records significant information regarding petroleum evolution, including hydrocarbon generation, migration, accumulation and alteration (Hwang et al., 1998; Parnell and Swainbank, 1990; Selby et al., 2005; Summons et al., 2008; Zhu et al., 2001). Recently, Re-Os isotope dating of oil and bitumen has shown good potential for determining the absolute timing of hydrocarbon generation (Cumming et al., 2014; Finlay et al., 2011; Ge et al., 2016; Georgiev et al., 2016; Lillis and Selby, 2013; Selby and Creaser, 2005; Selby et al., 2005; Selby et al., 2007). In this study, we present new Re-Os data and organic geochemistry of bitumen and present day oil seeps from the Northern Longmen Shan Thrust belt. The data are discussed with the previous hydrocarbon evolution knowledge, as well as U-Pb, Ar-Ar and Apatite Fission Track (AFT) dates that constrain the timings of tectonism to understand the petroleum evolution and its relationship with tectonism. Our data provide not only an improved understanding of the petroleum evolution within the Longmen Shan Thrust belt, but also provides implications for the potential utility of Re-Os hydrocarbon chronometer to help constrain the absolute timing of both hydrocarbon generation and associated tectonism in petroleum systems worldwide.

2. Geological Setting

The NE-SW striking Longmen Shan Thrust belt is ~500 km long and ~50 km wide. The belt is bordered by the Micang Shan uplift to the north, the Kangdian paleo uplift to the South, the Songpan-Garze Belt to the west, and the Sichuan Basin to the east (Burchfiel et al., 1995; Dirks et al., 1994; Jin et al., 2010) (Fig. 1C). Longitudinally, the Longmen Shan Thrust belt is divided into three sub-structural belts by four major faults: the Maoxian-Wenchuan, Beichuan-Yingxiu, Anxian-Dujiangyan and the Guangyuan-Dayi

faults (Fig. 1C). Further, the belt can also be separated geographically into three areas: the northern, middle and southern segments (Fig. 1C) (Chen and Wilson, 1996; Deng et al., 2012; Jin et al., 2010; Li et al., 2008; Liu et al., 2016; Wang et al., 2015; Yan et al., 2011).

The Longmen Shan Thrust belt has experienced a complex tectonic evolution since the Early Palaeozoic (Chen and Wilson, 1996; Dai, 2011; Jin et al., 2010; Yan et al., 2011). The initial tectonic events were associated with the Palaeozoic Caledonian Orogeny caused by the closure of the Tethys ocean, with thrusting causing numerous unconformities between the Early Palaeozoic strata (Jin et al., 2010). Following the Caledonian Orogeny (Early Devonian), the Longmen Shan belt changed into a passive continental margin throughout the Devonian and Permian that was associated with extensional tectonism (Jia et al., 2006; Li et al., 2012; Tian, 2009; Zhou et al., 2013). The most severe deformation recorded in the Longmen Shan thrust belt relates to the Late Triassic to Early Cretaceous NW to WNW directed under-thrusting of the South China block beneath the North China block (Chen and Wilson, 1996; Dai et al., 2009; Jin et al., 2010; Liu et al., 2005; Yan et al., 2011). These tectonic events resulted in structural unconfomities within the Triassic and between the Upper Triassic and Lower Jurassic strata (Tian, 2009), numerous faults (e.g., Beichuan-Yingxiu Faults, Anxian-Dujiangyan Faults and the high angle reverse fault in this study (Fig. 3B)) (Arne et al., 1997; Chen et al., 1995; Wilson et al., 2006), intensive folding of the Jurassic strata and led to the uplift and erosion of Cretaceous strata (Li et al., 2008). The absolute timing of tectonism is constrained by Sensitive High Resolution Ion Microprobe analysis (SHRIMP) U–Th–Pb monazite, conventional U-Pb titanite, Sm–Nd garnet, and Rb–Sr muscovite and biotite ages on metamorphic rocks from the Danba Domal Metamorphic

147 Terrane ~100 km northwest of the southern sector of the Longmen Shan Thrust Belt.
148 The available geochronology yield three age groups (ca. 200, ca. 160 and ca. 120 Ma)
149 (Huang et al., 2003; Jin et al., 2010; Jin et al., 2008; Yan et al., 2011). Further age
150 constraints for the timing of tectonism are given by $^{40}Ar/^{39}Ar$ garnet and zircon fission
151 track dates (ca. 110 - 130 Ma) from the middle district of the Longmen Shan Thrust Belt
152 (Liu et al., 2001), and $^{40}Ar/^{39}Ar$ muscovite and sericite dates (ca. 237 - 183 Ma) from
153 the basement complex, detachment fault zone and ductile deformation zone from the
154 northern part of the Longmen Shan Thrust Belt (Yan et al., 2011). The most recent
155 tectonism recorded by the Longmen Shan Thrust Belt occurred during the Cenozoic as a
156 result of the India-Asia continental collision (Dai, 2011; Li et al., 2008; Yan et al.,
157 2011). This event further reactived previous existing thrust faults and caused
158 exhumation along the belt (Harrowfield and Wilson, 2005; Lei et al., 2012; Yan et al.,
159 2011). Low-temperature thermochronology, such as apatite fission track (AFT) and (U-
160 Th)/He methods, indicate a series of uplift events since the Late Cretaceous (Arne et al.,
161 1997; Deng et al., 2012; Lei et al., 2012; Yan et al., 2011). Additionally, present day
162 activity along the Longmen Shan Thrust Belt is evidenced by the 2008 Wenchuan
163 earthquake (7.9 M_w – epicentre in Wenchuan City) and the 2012 Ya'an earthquake (6.6
164 M_w – epicentre in Ya'an City) (Feng et al., 2014).
165 The northern segment of the Longmen Shan Thrust Belt, located to the north of Anxian
166 County, extends for ~200 km (Fig. 1C). This segment of the belt contains several major
167 thrust sheets and a blind frontal thrust zone, with most of the folds and thrust sheets
168 emplaced towards the southeast (Jia et al., 2006; Jin et al., 2010; Jin et al., 2009a).
169 Precambrian to Quaternary strata are present in the northern Longmen Shan Thrust Belt
170 (Jia et al., 2006; Jin et al., 2009a). The Precambrian to Cambrian units mainly consist of

organic-rich black shales and siltstones with a total thickness of ~200 m (Rao et al., 2008; Wang et al., 2005; Xie et al., 2003). The Ordovician to Silurian units are largely absent due to uplift and erosion during the Caledonian Event (ca. 450 – 400 Ma) in the Yangtze Block. Devonian and/or Carboniferous strata, which mainly consist of dolomite and limestones, uncomformably overlie the older units and possess a thickness ~50 – 250 m. The Permian strata, which have a total thickness ~270 - 470 m, consist of limestone and black shales (Rao et al., 2008; Wang et al., 2005; Xie et al., 2003). The Early-Mid Triassic strata include ~750 m of limestones interbedded with sandstones or shales. The Late Triassic units of ~400 m thickness comprise interbedded sandstones and mudstones (Zhou et al., 2013). The overlying Jurassic and Cretaceous fluviolacustrine sediments comprise mudstones, sandstones and siltstones with a total thickness of up to 4500 m (Fig. 2).

The Upper Neoproterozoic to Lower Cambrian shales and middle Permian black mudstones are considered as the potential source rocks (Xie et al., 2003; Zhou et al., 2013) to several petroleum systems (e.g., Ningqiang, Tanjingshan and Kuangshanliang) in the northern Longmen Shan Thrust Belt (Chen et al., 1994; Huang and Wang, 2008; Tissot and Welte, 1984). Reservoir units include the Upper Cambrian, Lower Devonian, Lower and Upper Permian, Lower Triassic and Upper Jurassic carbonates, sandstones and/or siltstones (Chen and Wilson, 1996; Li et al., 1999; Worley and Wilson, 1996; Zhou et al., 2013). Devonian marine mudstones, Triassic gypsum, and Jurassic to Cretaceous mudstones act as seals to the several petroleum systems (Zhou et al., 2013) (Fig. 2).

The Kuangshanliang petroleum system is characterized by the largest and most complete anticline in the frontal thrust zone of the northern Longmen Shan Thrust Belt

(Fig. 3A) (Chen et al., 2005). The anticline comprises Cambrian strata in the core, surrounded by Ordovician to Triassic units (Fig. 3A). Bitumen and present day oil seeps in the Kuangshanliang anticline occur in the 565 m thick marine clastics of the Lower Cambrian Changjianggou Formation (Fig. 3A, B) as dykes or along faults and/or fractures that trend NW-SE. The calculated total hydrocarbon reserves in the Kuangshanliang anticline are ~70 Mbbl of oil (Tian, 2009).

3. Samples

Bitumen and oil seep samples were collected between 2010 and 2011 from field outcrops of bitumen dykes, fault planes, fault zones, fractures and seeps, in the Cambrian Changjianggou Formation (Figs. 3, 4). The densely forested nature of the area has resulted in there being no known outcrops of the bitumen dykes. The bitumen dykes were only accessible through old mine adits. Samples were obtained through three old mine adits approximately 8 km north of Shangsi, Jiange County (Fig. 3A). Access to these adits has been prohibited since 2012 for health and safety reasons. The dykes are ~0.5 - 10 m wide and occur over a known strike (NW) distance of ~50 m. The dykes typically run parallel to faults that show a dextral motion and dip ~35º towards the southwest. The contacts between the bitumen dykes and the country rock are sharp, although bitumen also impregnates the wallrocks up to ~10 cm from the edge of the dyke.

Two dykes (Dykes 1 and 2) are located within ~500 m of each other. Dyke 1 was accessed from the mine adit Shang Kuang Dong (upper bitumen hole). The dyke strikes NW over a distance of at least 100 m, and averages a width of 70 - 100 cm. The eastern contact with the Cambrian Changjianggou Formation sandstone is sharp, but the

219 western contact is brecciated (Fig. 4A). The breccia zone is ~10 cm wide and contains 1
220 - 5 mm clasts of both the country rock (sandstone) and bitumen. Inward from the
221 brecciated area, the western edge of Dyke 1 is intensively fractured over 10-20 cm.
222 Three bitumen samples (11SKD-3d, 11SKD-4d and 11SKD-5d) were taken, ~2 m apart,
223 from the centre of the dyke, which represents the least fractured part of Dyke 1 (Fig.
224 4B). A fourth sample (SKD-1f) was taken from a cross-cutting bitumen-filled fracture
225 (Fig. 4B). Dyke 2 was accessed from mine adit Xia Kuang Dong (lower bitumen hole).
226 Two bitumen samples (XKD-1d; XKD-2d) were collected from the center of this dyke,
227 ~5 m apart (Fig. 4C). Dyke 2 is narrower than Dyke 1 (20 - 50 cm), and strikes NW for
228 at least 100 m. Both the western and eastern contacts with the host rock are sharp, with
229 the adjacent country rocks being impregnated with bitumen up to 10 cm from the
230 contact. In contrast to Dyke 1, the eastern margin of Dyke 2 is part of a low-angle
231 reverse fault (Fig. 4C). The fault plane strikes NE and dips 34º to the NNW, with
232 transport direction towards the SE. These fault characteristics are consistent with the
233 overall pattern and geometry of thrusting in the northern Longmen Shan Thrust belt
234 (Chen et al., 2005; Tian, 2009). The fault plane and associated gouge is confined to a 5
235 cm thick, clay-rich siltstone interbed of the Cambrian Changjianggou Formation
236 sandstone. The gouge has a sharp upper contact and diffuse basal contact. The bitumen
237 impregnated into the sandstone country rock indicates a SE-ward fault motion syn-post
238 emplacement of the bitumen Dyke 2 (Fig. 4D).
239 Seven additional bitumen samples (GY1d-6d and HSCD-1d) were collected from a third
240 Dyke (Dyke 3) from the Huoshicun mine hole, ~2 km to the south of Dykes 1 and 2.
241 Samples in Dyke 3 were collected along the centre of the main bitumen dyke body (Fig.
242 4E). Dyke 3 has a similar strike orientation to that of Dykes 1 and 2 (NW), and

243 possesses a similar width to Dyke 2 (30 – 50 cm). Both the eastern and western dyke
244 contacts are sharp, with little to no bitumen impregnated into the sandstone, and with no
245 evidence of post-emplacement fracturing or faulting observed.
246 In the Northern Longmen Shan Thrust Belt, dextral strike-slip faults striking NE and
247 dipping 30-40º NW are well developed (Burchfiel et al., 1995; Chen et al., 2005; Yan et
248 al., 2011). In this study, the bitumen samples were also collected from two separate
249 faults (Fig. 4F,G). Samples LXB-1f and LXB-2f were collected from the same fault,
250 which strikes NE and dips 75º NW (Fig. 4F). The samples were taken ~2 m apart.
251 Sample 11LXB-1f was collected from part of a slickenline striking NE with a dip of 45º
252 NNW (Fig. 4G).
253 At the Huoshicun mine hole, oil was observed seeping through the Changjianggou
254 Formation sandstone, three oil samples (Oil-3, Oil-5, Oil-7) were collected over a
255 distance of 1 m (Fig. 4H).
256
257 **4. Analytical Protocols**
258 The Gas Chromatography (GC) and Gas Chromatography-Mass Spectrometry (GC-MS)
259 analyses on nine bitumen samples (GY-1, 3, 5, 11SKD-4, 11LXB-1, HSCD-1, SKD-1,
260 XKD-1 and LXB-1) and two present day oil seep samples (Oil-3 and Oil-5) were
261 conducted in Wuxi Institute of Petroleum Geology, Sinopec, China and Weatherford
262 Laboratories, USA, following the analytical procedure of Hackley et al., 2013 . The
263 bitumen samples were first cleaned with distilled water, to ensure there were no
264 weathered contaminants on the surface, and then crushed to 100 mesh size using an
265 agate pestle and mortar. Approximately 100 g of bitumen was put into a Soxhlet
266 extractor for 72 hours to obtain the chloroform extract (asphalt). The asphalt was then

267 precipitated using n-hexane. For the oil samples, ~30 mg of crude oil sample was
268 dissolved in 50 mL of *n*-hexane and left for 12 h at room temperature. The solution was
269 then filtered, with all the filtrates collected and evaporated under nitrogen gas to 0.5 mL.
270 A chromatographic column (30 cm × 10 mm in diameter) was prepared using a mixed
271 stationary phase of activated silica gel and alumina at a ratio of 3:2 by referring to
272 relevant literature (e.g., Yang et al., 2009). The concentrated sample was transferred to
273 the chromatographic column for further separation. The saturated hydrocarbon fraction
274 was eluted with *n*-hexane (25 mL). The fractions were then carefully concentrated under
275 nitrogen flow to 0.5 mL for GC-MS analysis. The GC-MS system consisted of an
276 Agilent 7890 GC, and an Agilent 5975C mass spectrometer. A DB-5MS column 50 m ×
277 0.25 mm × 0.25 μm was used. High purity helium (99.9995%) was used as a carrier gas
278 at a flow rate of 1.0 mL/min. The injector temperature was 300°C. The injection volume
279 was 1.0 L. All injections were done with a 7683B series autosampler. The oven
280 temperature was programmed from 50°C (1 min hold) to 100°C at 10°C /min, and then
281 to 310°C (20 min hold) at 2°C /min. The mass spectrometer was operated in the electron
282 impact mode (70 eV). The temperature of ion source and transfer-line were set at 230°C
283 and 300°C, respectively. The scanned mass range was from 50 to 550 u. The
284 temperature of the Quadrupole was held at 150°C.
285 For Re-Os analysis, approximately ~0.2 - 1.0 g bitumen was separated from the 16
286 samples. All samples were isolated without metal contact and handpicked. Samples
287 were crushed to ~1 mm grains using an agate pestle and mortar. For the oil seeps, the
288 asphaltene fraction was analyzed as Re and Os are predominantly contained within the
289 asphaltene fraction of oil (Selby et al., 2007). The asphaltenes were precipitated from
290 the oil using 40 times volume of *n*-heptane (~1 g oil with 40 ml solvent) at room

291 temperature for at least 8 hrs. The asphaltene abundance of the present day oil seeps are
292 between 9.48 and 13.54 % (Table 1). The Re and Os isotopic compositions, and
293 abundances of the bitumen and asphaltene from the oil were analysed at the Laboratory
294 for Source Rock and Sulfide Geochronology and Geochemistry (a member of the
295 Durham Geochemistry Centre) at Durham University following published analytical
296 procedures (e.g. Selby et al., 2005; Selby et al., 2007). Approximately 100 - 200 mg of
297 bitumen or asphaltene were dissolved and equilibrated with a known amount of ^{185}Re
298 and ^{190}Os spike solution by inverse *aqua-regia* (3 ml HCl and 6 ml HNO_3) in a Carius
299 tube for 24 hours at 220˚C. Osmium was isolated and purified from the inverse *aqua-*
300 *regia* by $CHCl_3$ solvent extraction at room temperature and micro-distillation. The Re
301 was isolated using HCl-HNO_3 based anion chromatography. The purified Re and Os
302 were loaded on Ni and Pt filaments and analyzed using Negative Ion Thermal Ionization
303 Mass Spectrometry (N-TIMS). Measured Re and Os ratios were corrected for mass
304 fractionation using $^{185}Re/^{187}Re$ = 0.59738 (Gramlich et al., 1973) and $^{192}Os/^{188}Os$ =
305 3.08261, spike and blank contributions. All data were blank corrected based on the total
306 procedural blanks values of Re (1.6 ± 0.025 pg) and Os (0.05 ± 0.004 pg), with an
307 average $^{187}Os/^{188}Os$ ratio of ~0.22 ± 0.06 (n = 4). All uncertainties include the
308 propagated uncertainty in the standard, spike calibrations, mass spectrometry
309 measurements, and blanks. In-house Re (Restd) and Os (AB2) solutions were analyzed
310 as a monitor of reproducibility of isotope measurements. The analyses presented in this
311 study were conducted prior to using DROsS as our in-house control solution (Nowell et
312 al., 2008). The $^{187}Os/^{188}Os$ values of the Os standard solution AB2 during this study
313 were 0.1611 ± 0.0066, with the $^{185}Re/^{187}Re$ values of the Re standard solution being
314 0.5984 ± 0.0002. These values are in agreement with those previously published for

AB2 and Restd (Cumming et al., 2014; Finlay et al., 2011, 2012; Lillis and Selby, 2013; Rooney, 2011). The $^{185}Re/^{187}Re$ ratios for samples of this study were corrected for the measured difference of the $^{185}Re/^{187}Re$ value for Restd and the $^{185}Re/^{187}Re$ value of 0.59738 ± 0.00039 (Gramlich et al., 1973). The Re–Os data of this study are regressed using the program *Isoplot* V. 4.15 (Ludwig, 2003) with ^{187}Re decay constant of $1.666\times10^{-11}a^{-1}$ (Smoliar et al., 1996). The input data contains $^{187}Re/^{188}Os$ and $^{187}Os/^{188}Os$ ratios with their total 2σ uncertainty and associated error correlation, Rho.

5. Results

This study presents results of organic geochemistry for nine bitumen and two present day oil seeps, and Re-Os data for the sixteen bitumen samples and three present day oil seeps. The detailed results of the organic geochemistry and Re-Os analysis are presented below.

5.1 GC-MS results

Nine samples from the three bitumen dykes and bitumen from faults/fractures were selected for detailed organic geochemistry analysis (Table 1). Component analysis show that the asphaltene fraction occupies more than 98 % of the total bitumen sample (Table 1). The saturate fraction gas chromatograms (SFGCs) of the analyzed bitumen samples are dominated by humps of unresolved compounds (UCM) with some discrete peaks superimposed (Fig. 5). The UCM exhibited by the SFGCs indicates that the samples have been extensively biodegraded with compounds, such as *n*–alkanes and acyclic isoprenoids, removed by microbial action. This is also supported by the presence of Nor-25-hopane (Wenger and Isaksen, 2002) (Fig. 5). Gas chromatograms show that the

Carbon Preference Index (CPI) value based on the formula (NC23+NC25+NC25)+ (NC25+NC27+NC29)/(2*(NC24+NC26+NC28)) ranges from 0.35 to 2.59, with majority of samples possessing CPI values between ~0.91 and 1.21 (except LXB-1f and HSCD-1d). The calculated Pr/Ph ratio for samples 11SKD-4d (Dyke 1), XKD-1d (Dyke 2) and HSCD-1d (Dyke 3) range form 0.47 to 0.95. The bitumen samples show peak values for tricyclic terpanes (C_{19} to C_{30}) at C_{21} or C_{23} (Fig. 5). The C_{23}/C_{21} tricyclic terpane values range from 0.89 to 1.67, with an average of 1.35. The C_{24} tertracyclic/C_{26} tricyclic terpane ratios range from 1.00 to 2.61, with only two samples (11SKD-4 and SKD-1) possessing ratios >2.0 (Table 1). The hopanes (C_{27} to C_{35}) exhibit peaks at C_{29} or C_{30} (Fig. 5). The abundance of the C_{31} to C_{35} hopanes decrease with increasing carbon number. In addition to the presence of C_{30} diahopane, Ts (18α(H)-trisnorhopane), and Tm (17α(H)-trisnorhopane), and gammacerane are also detected (Fig. 5). The Ts/(Ts+Tm) values range from 0.20 to 0.38, with an average of 0.31, DH_{30}/H_{30} values range from 0.02 to 0.08, with an average of 0.05, and C_{32} hopane S/(S+R) values range from 0.54 to 0.62, with an average of 0.58. The bitumen samples yield a gammacerane index of 0.12 to 0.22, with an average of 0.16. The ratio of Nor-25-hopane/hopane range from 0.07 to 0.19, with the exception of sample SKD-1f, which has a ratio of 0.07, all other samples possess a similar ratio (0.15).

Sterane compounds including C_{21} pregnane, C_{22} sterane, diasterane and C_{27}-C_{29} sterane were also detected (Fig. 5). The ratio of S_{21}/S_{22} range from 2.36 to 2.58, with an average of 2.44. C_{27}, C_{28}, C_{29} steranes of all the bitumen display a similar V-shape distribution which occupy ~30.2, 16.0 and 53.8 %, respectively, with C_{29} sterane exhibiting the highest abundance. The ratio of C29ααα20S/(20S+20R) and C29ββ/(ββ+αα) vary from 0.46 to 0.52 and 0.49 to 0.57, respectively, which yield a similar Ro value (~0.9). The

organic geochemistry of the bitumen samples analyzed in this study suggest that all the bitumen has middle to high maturity, and was sourced from similar organic matter derived from marine algae deposited in an anoxic environment (De Grande et al., 1993; Didyk, 1978; Peters et al., 2005; Seifert and Moldowan, 1986).

However, the organic analysis of two of the present day oil seep samples (Oil-3 and Oil-5) show very different organo-geochemical features as compared to the bitumen. This observation is critical given that these samples are taken in close spatial (~20 m) proxmity to the bitumen samples GY-6 and HSCD-1, which suggests that the organo-geochemical characteristics of the bitumen have not been appreciably affected by the present oil seeps. The SFGCs display UCM and suggest severe biodegradation of the present day oil seeps (Fig. 5). Given the lack of the majority of the *n*-alkanes, the data related to CPI or Pr/Ph values can not be calculated. Terpanes and hopanes, except for the Ts/(Ts+Tm) ratio (0.31 vs 0.36), of the oil are similar to the bitumen. Further, all of the other parameters, for example gammacerane/hopane (3.91-7.59), C_{24} tertracyclic/C_{26} tricyclics (0.51-0.52) and DH_{30}/H_{30} (3.10-5.54) values are distinctly different in comparison to the bitumen samples (Table 1). Only C_{21} and C_{22} steranes in the oil were dectected, which yield a S_{21}/S_{22} ratio of 0.21 and 0.20, respectively, which are also different as compared to the bitumen. The limited organic data for the present day oil seep samples suggests that the organic fraction of the oil is derived from a source rock deposited in a hypersaline, suboxic and clay-rich environment (Peters and Moldowan, 1993; Zumberge, 1987).

5.2 Re-Os results

The Re and Os abundances of all the bitumen samples range between 283.1 and 547.9

ppb, and 4.06 and 15.3 ppb, respectively (Table 2). These values are significantly elevated from those of the average continental crust (Esser and Turekian, 1993), but similar to previously reported bitumen samples, and the organic-rich sedimentary rocks (Cohen et al., 1999; Esser and Turekian, 1993; Georgiev et al., 2016; Ravizza and Turekian, 1992; Rooney et al., 2010; Selby and Creaser, 2005; Xu et al., 2009; Xu et al., 2014). The $^{187}Re/^{188}Os$ values of the bitumen range from 229.5 to 595.1 and exhibit a radiogenic $^{187}Os/^{188}Os$ composition of 2.79 to 3.56 (Table 2). Repeat analyses of a single bitumen sample (11SKD-4d-rpt) yield highly reproducible (<1%) Re (~512.2 ± 1.8 vs 518.8 ± 1.3 ppb) and Os (14478.3 ± 46.3 vs 14605.3 ± 75.8 ppt) concentrations, and $^{187}Re/^{188}Os$ (230.7 ± 0.9 vs 231.5 ± 1.0) and $^{187}Os/^{188}Os$ (2.84 ± 0.01 vs 2.83 ± 0.01) values (Table 2). Similar reproducibility has been shown by previous studies (Lillis and Selby, 2013; Selby et al., 2005).

Collectively the bitumen Re-Os isotope data from the three dykes, fault and fracture surfaces does not show any linear relationship, and shows a large range in isotope compositions (Fig. 6A). Herein we discuss the Re-Os data of each bitumen occurrence separately. The three samples from Dyke 1 have extremely similar Re-Os isotope compositions, and as a result do not yield a meaningful Re-Os date (674 ± 490 Ma). Bitumen from a fracture (SKD-1f) that postdates Dyke 1 exhibits broadly similar $^{187}Os/^{188}Os$, but higher $^{187}Re/^{188}Os$ values than that of the dyke (Table 2). The two bitumen samples from Dyke 2 show distinctly different Re-Os isotope compositions in comparison to Dyke 1, specifically with respect to the $^{187}Re/^{188}Os$ values. Although, dates derived from only two samples may not be completely reliable geologically, the Re-Os data from the two Dyke 2 bitumen samples may suggest that bitumen formation occurred during the Early Jurassic (181 ± 41 Ma). Bitumen from Dyke 3 exhibit the

largest variation in Re-Os isotope space, with the compositions specifically different to Dyke 1 (with the exception of GY-5d) and Dyke 2. The Re-Os data of Dyke 3 yield a Model 3 (which assumes that the scatter in the degree of fit of the data is a combination of the assigned uncertainties, plus a normally distributed variation in the $^{187}Os/^{188}Os$ values (Ludwig, 2003)) date of 503 ± 140 Ma (Mean Squared Weighted Deviation, MSWD = 90), with an initial $^{187}Os/^{188}Os$ value of 0.91 ± 0.71 (Fig. 6B). The Re-Os date and its uncertainty is largely controlled by sample GY-5d that controls the lower anchor of the best-fit line of the data, and HSCD-1 and GY-1d which plot above the best-fit line, respectively. Using the Re-Os date of 503 Ma to calculate the initial $^{187}Os/^{188}Os$ (Os_i) values, shows that samples HSCD-1 and GY-1d possess Os_i values (~1.0) that are slightly more radiogenic than the samples GY-2d, 3d, 4d, 5d, and 6d (0.85 - 0.89), and we consider that the samples HSCD-1 and GY-1d are the principal controls on the Re-Os date and uncertainty (Table 2). Considering only the samples (GY-2d, 3d, 4d, 5d, and 6d) that possess similar Os_i values, the Re-Os data yield a more precise Re-Os date of 483 ± 27 Ma, with an Os_i value of 0.97 ± 0.13.

The Re-Os isotope data of bitumen sampled from faults and fractures show no linear trends. Sample 11LXB-1f possesses similar $^{187}Re/^{188}Os$ and $^{187}Os/^{188}Os$ values to those of Dyke 3, specifically GY-3d and 4d. In contrast, the Re-Os data of SKD-1f, LXB-1f and 2f are similar to that for Dyke 2. Combined, the bitumen Re-Os data of Dyke 2 and from the fractures represented by samples SKD-1f, LXB-1f and 2f define a broadly positive correlation between the $^{187}Re/^{188}Os$ and $^{187}Os/^{188}Os$ compositions, and yield a Re-Os date of 158 ± 76 Ma, with an Os_i value of 1.85 ± 0.61 (MSWD = 79) (Fig. 6E). The uncertainty in this date is because samples (LXB-1f, SKD-1f, LXB-2f, XKD-2d) though very close to the linear regression, still deviate from the line of best-fit. The Os_i

values calculated at 158 Ma show that samples LXB-1f and SKD-1f possess less radiogenic Os_i values (1.80 and 1.75) in comparison to XKD-1d, XKD-2d and LXB-2f (1.87 to 1.91) (Table 2). Treated separately the Re-Os data for samples XKD-1d, XKD-2d and LXB-2f, and samples LXB-1f and SKD-1f record a Mid Jurassic age (162 ± 14 Ma, with an Os_i value of 1.87 ± 0.12, and 172.6 ± 8.1 Ma, with an Os_i value of 1.66 ± 0.06, respectively) (Fig. 6F).

The present day oil seep samples possess very different Re-Os systematics as compared to all the bitumen samples. In contrast to the bitumen samples the asphaltene fractions of the oil seep samples possess much lower Re and Os abundances (Re of 7.7 to 9.6 ppb, Os of 90.3 to 127.2 ppt) (Table 2). The $^{187}Re/^{188}Os$ and $^{187}Os/^{188}Os$ values of the oils are very similar, 496.3 to 579.3 and 2.89 to 2.93, respectively (Table 2). As the three oil seep samples possess very similar Re and Os isotope compositions, no meaningful Re-Os date can be determined.

6. Discussion

6.1 Bitumen and Oil Geochemistry and source tracing

In this study, the biomarker analysis shows that all the bitumen from the dykes, fractures and faults possess similar organo-geochemical characteristics, distinct from the present day oil seeps. The bitumen molecular compostition (*n*-alkanes, terpanes and steranes) are interpreted to suggest that the bitumen organic matter derived from a marine source deposited in an anoxic setting, are mature (Ro: ~0.8 - 1.0) and biodegraded (Pr/Ph ratio = 0.47-0.95; Gammacerane/H30 = ~0.16; C_{23}/C_{21} tricyclic = ~1.35; C_{24} tertracyclic / C_{26} tricyclics = ~1.41; Ts/(Ts+Tm) = ~0.31; diahopane/hopane = ~0.05 and H_{32} S/(R+S) homohopane = ~0.58; the 25-nor-hopane/hopane = ~0.15)

(Table 1) (Peters and Moldowan, 1993; Wenger and Isaksen, 2002; Zumberge, 1987). Further, the sterane chromatogram (m/z = 217), pregnane/homopregnane ratio (~2.44), as well as the V-shape C_{27}-C_{29} sterane distribution, with C_{29} being the largest component, implies that all the bitumen in the study area is derived from the same source rock (e.g. Peters and Moldowan, 1993; Wu et al., 2012). The C29 ααα S/(S+R) and C29 ββ/(ββ+αα) ratios (0.49 and 0.53, respectively) also indicate that the bitumen was generated during peak oil generation (Georgiev et al., 2016; Peters and Moldowan, 1993).

In comparison to the bitumen samples the present day oil samples are severely biodegraded and are slightly less mature (Ts/Ts+Tm ratio = 0.36) (Table 1; Fig. 5). The remaining biomarker parameters (gammacerane/hopane = 7.59 and 3.91; C_{24} tertracyclic/C_{26} tricyclics = 0.52; diahopane/hopane = 5.54 and 3.10; pregnane/ homopregnane = 0.21) are supportive of the organo-geochemical signature of the present day oil seeps being derived from the organic matter deposited in a sub-oxic marine-continental sedimentary environment (Peters and Moldowan, 1993; Zumberge, 1987). The Late Neoproterozoic to Early Cambrian Doushantuo and Qiongzhusi formations and the Upper Permian Dalong Formation are considered to be the principal source rocks in the Kuangshanliang area (Huang et al., 2011; Lin et al., 2011; Liu et al., 2009; Sun et al., 2009; Wei et al., 2008). Previous work shows that the geochemical parameters of both C_{23} tricyclics/C_{24} tertracyclic and pregnane/homopregnane are higher (>2.5 and ~2.0) for the Late Neoproterozoic-Early Cambrian formations than for the Upper Permian Dalong Formation (<1.6 and ~1.0) (Wu et al., 2012). In this work, the C_{23} tricyclics/ C_{24} tertracyclic and pregnane/homopregnane ratio of the bitumen samples are respectively ~2.42 and ~2.44, however, for the present day oil seep samples,

these organic parameter ratios are only ~0.25 and 0.20 (the ca. 5 times lower ratio compared with Permian mudstone may be caused by the biodegradation of the present day oil seeps). Given that hydocarbons possess similar biomarker characterisitcs to that of its source unit (Cole et al., 1987; Pusey, 1973; Wu et al., 2012; Zhang et al., 2000), the results of this study suggest that the bitumen and oil seeps are sourced from different units, with the bitumen being sourced predominantly from the shales of the Late Neoproterozoic Doushantuo and Early Cambrian Qiongzhusi formations, and the present day oil seeps from the mudstones of the Permian Dalong Formation. The identification of the Doushantuo and Qiongzhusi formations being the source of the bitumen in the Kuangshanliang area further supports the oil-source correlation based on the similar $\delta^{13}C$ values for bitumen and the Doushantuo and Qiongzhusi formations (bitumen = -35.71 ‰ to -27‰ (Wu et al., 2012; Zhou et al., 2013); Precambrian-Cambrian = -30.3‰ to -35.4‰; (Wu et al., 2012; Zhou et al., 2013)), in contrast to the oil and Dalong Formation (oil = -25.9‰ to -27.7‰ (Wu et al., 2012); Permian Dalong Formation = -25.9‰ to -27.7‰ (Liang, 2007; Zhou et al., 2013)).

6.2 Multiple phases of petroleum generation

Previous studies suggest that oil generation in the North Longmen Shan Thrust Belt and the adjacent Sichuan Basin is a result of the hydrocarbon maturation of the Late Neoproterozoic - Early Cambrian shales (e.g., Late Neoproterozoic Doushantuo and Early Cambrian Qiongzhusi formations) during the Middle Ordovician (Zhou et al., 2013; Zou et al., 2014b). The only Re-Os dataset that provides a robust estimation of oil generation during the Ordovician is the bitumen from Dyke 3. As discussed above, all the Re-Os bitumen from Dyke 3 yield a Model 3 date of 503 ± 140 Ma (Fig. 6B).

However, considering only the Re-Os bitumen data of Dyke 3 that possess similar Os_i values (GY-2d, 3d, 4d, 5d, and 6d; Os_i = 0.85 - 0.89) calculated at 503 Ma, a Re-Os date of 483 ± 10 Ma is determined. The absolute reason why the samples HSCD-1 and GY-1d possess slightly elevated Os_i values (~1.0) in comparison to the majority of the bitumen from Dyke 3 is not known. But the reasoning could be related slight post-depositional disturbance to the Re-Os systematics and/or continuous hydrocarbon generation. Both determined Re-Os ages are in agreement within uncertainty, with the more precise age determined, by the bulk of the sample set, providing an age that agrees well with modeling for the timing of burial (~2500 m and ~100 ºC) and source rock maturation of the Doushantuo and Qiongzhusi formations in the Northern Longmen Shan Thrust Belt and adjacent Sichuan Basin (Liu et al., 2009; Yuan et al., 2012; Zhou et al., 2013).

In contrast to Dyke 3, the bitumen Re-Os data from Dyke 1 yield no meaningful age because of the limited spread in $^{187}Re/^{188}Os$ and $^{187}Os/^{188}Os$ values. However, the bitumen Re-Os isotope compositions of Dyke 1 are similar to that of sample GY-5d from Dyke 3 (Table 2). Calculated at the age of Dyke 3 (483 Ma), the Re-Os bitumen data of Dyke 1 yield Os_i values (0.96-0.99) which is similar to the range of that determined for Dyke 3 (0.96 - 0.98; except GY-1 and HSCD-1) (Table 2). Based on the similarity of the GC-MS (e.g., m/z 191 and 217; Fig. 5) and Re-Os data of bitumen from the Dyke 1 and Dyke 3, we consider the bitumen to be of the same oil generation episode. Together, the Re-Os data from both Dyke 3 (except GY-1 and HSCD-1) and Dyke 1 yield a Model 3 date of 486 ± 15 Ma (Fig. 6D).

In comparison to the bitumen from Dyke 1 and 3, the Re-Os characteristics of the five bitumen samples from Dyke 2 and faults/fractures have very different Re-Os

systematics. Calculated at 486 Ma the Re-Os data of Dyke 2 and faults/fractures yield negative $^{187}Os/^{188}Os$ values (-0.05 to -1.04; Table 2). Furthermore, relative to a ca.486 Ma reference isochron, the five samples of Dyke 2 and faults/fractures have higher $^{187}Re/^{188}Os$ ratios for a given $^{187}Os/^{188}Os$ (Fig. 6E). This suggests that these bitumen samples are either of a different generation age to that of Dyke 1 and 3, or the Re-Os bitumen systematics of the Dyke 2 and faults/fractures have been disturbed.

The Re-Os data of the five bitumen samples from Dyke 2 (XKD-1d, XKD-2d) and fault/fractures (SKD-1f, LXB-1f, LXB-2f) together yield a Model 3 Re-Os date of 158 ± 76 Ma ($^{187}Os/^{188}Os$ = 1.85 ± 0.61, MSWD = 79) (Fig. 6E). For the Re-Os isotope compositions (e.g., $^{187}Re/^{188}Os$ and $^{187}Os/^{188}Os$) to yield a statistically meaningful isochron date, the samples comprising the dataset must have formed contemporaneously, must possess the same initial ($^{187}Os/^{188}Os$) isotope ratio, and the isotope systematics must not have been affected post formation (Cohen et al., 1999; Kendall et al., 2009; Selby et al., 2007). For these five bitumen samples, the degree of scatter about the best-fit line of the data, as given by the MSWD, is 76. The high MSWD indicates that one of the criteria for developing a statistically meaningful isochron has not been met. Although post-depositional effects, diffrerent sample localities, and contemporaneity between the sample set may affect the Re-Os data, the positive correlation of the Re-Os data may indicate that the major reason for the scatter could be a result of variable initial $^{187}Os/^{188}Os$ values. Using the Re-Os date derived by the isochron (158 Ma), initial $^{187}Os/^{188}Os$ values (Os_i) yield two populations for the sample set: (1) three samples with Os_i values of ~1.89 (samples XKD-1d, XKD-2d, LXB-2f); and (2) two samples with Os_i values of ~1.77 (samples SKD-1f; LXB-1f) (Table 2). Considering the sample set as two distinct populations, the three bitumen samples (XKD-1d, XKD-2d, LXB-2f) yield

555 a Model 1 Re-Os date of 162 ± 14 Ma (Os_i = 1.87 ± 0.12; MSWD = 0.95; Fig. 6F).
556 Although only two samples, the Re-Os data for bitumen samples SKD-1f and LXB-1f
557 define Re-Os date of 172.7 ± 8.1 Ma (Fig. 6F). Both the Re-Os dates are within
558 uncertainty and suggest that these five bitumen formed broadly contemporaneously
559 during the Middle Jurassic at 162 - 173 Ma.
560 The $^{187}Os/^{188}Os$ composition of an hydrocarbon at its time of generation is inherited
561 from its source (Finlay et al., 2011; Lillis and Selby, 2013; Selby and Creaser, 2005;
562 Selby et al., 2005; Selby et al., 2007). The difference in the initial $^{187}Os/^{188}Os$
563 compositions of the two temporally distinct bitumen samples (~0.95 vs ~1.85; Fig. 6;
564 Table 2) could indicate the bitumen could have been derived from different source rocks.
565 However, the organic geochemistry for all the bitumen samples are indicative of the
566 source rock being the Late Neoproterozoic to Early Cambrian Doushantuo and
567 Qiongzhusi formations. As such, the more radiogenic initial $^{187}Os/^{188}Os$ compositions of
568 bitumen formed during the Jurassic (~1.85) is the result of the greater duration of
569 radioactive ingrowth of ^{187}Os from the decay of ^{187}Re in the source rock since its
570 deposition. Although no Re-Os data was obtained for the potential source rock samples
571 in this study, Re-Os data of the Late Neoproterozoic – Early Cambrian shales from the
572 South China Block (Yangtze Gorges area (Kendall et al., 2009) and Zunyi, Guizhou
573 province (Jiang et al., 2007)) yield Os_i values at ca. 485 Ma and ca. 165 Ma of 0.89 -
574 0.98 and 1.54 - 2.01, respectively. The bitumen Os_i values at ca. 486 Ma and ca. 165 Ma
575 in this study all fall into this range, which further supports the bitumen are derived from
576 the same source, but during two separate phases of oil generation.
577 The Longmen Shan Thrust Belt records a series of complex tectonic events since the
578 Palaeozoic (Chen and Wilson, 1996; Dai, 2011; Jin et al., 2010; Yan et al., 2011). Burial

579 history models (Zhou et al., 2013; Zou et al., 2014b) coupled with the Re-Os dates of
580 the Dykes 1 and 3 suggest that oil generation of the Late Neoproterozoic Doushantuo
581 and Early Cambrian Qiongzhusi formations in the Northern Longmen Shan Thrust Belt
582 and the adjacent Sichuan Basin occurred during the Middle Ordovician. Oil generation
583 ceased during the Caledonian Orogeny (~450 – 400 Ma) due to more than 2000 m of
584 uplift and denudation (Wang et al., 1989; Wang et al., 2007; Zhuang, 1985; Zou et al.,
585 2014b). The maturation history of the Early Cambrian Qiongzhusi Formation based on
586 five different wells across the southwest Sichuan Basin indicates that the shales did not
587 enter the oil window between the Late Devonian and Carboniferous (Liu et al., 2009).
588 However, since Triassic, the Northern Longmen Shan Thrust Belt has been affected by
589 the Indosinian–Yanshan orogenies following the collison between the North and South
590 China blocks (Liu et al., 2005). Compressional tectonics in the Longmen Shan Thrust
591 Belt and Sichuan Basin continued into the Late Jurassic from the paleogeography model
592 (Jin et al., 2009b; Liu et al., 1996); apatite fission track date of 162 ± 23 Ma (Arne et al.,
593 1997); and post-tectonic granitoid magmatism at ~160 Ma (Jin et al., 2008) (Fig. 7). The
594 sheared bitumen accummulations observed in the sandstone country rock (Fig. 4D) also
595 suggests that the bitumen emplacement of Dyke 2 may be syn-tectonic. The Re-Os dates
596 (ca.162 - 172 Ma) of the five bitumen samples from Dyke 2 and fault/fractures coincide
597 with the timing of the tectonism in the Longmen Shan Thrust Belt during the Jurassic.
598 The organic geochemistry of the Dyke 2 and fault/fracture bitumen suggest that it is
599 sourced from the Late Neoproterozoic – Early Cambrian Doushantuo and Cambrian
600 Qiongzhusi formations. These units were buried to more than 5000 m and re-entered the
601 oil window (Ro ~1.2 %) during the Middle Jurassic (Liu et al., 2009; Zou et al., 2014b).
602 The hydrocarbon generation intensity of the Cambrian source rock units from the

603 Yangtze block (China) indicates that the Triassic and Middle Jurassic were the two peak
604 oil generation intervals (Liang, 2007). Further, analysis on the Zi 1 and Gaoke 1 Wells
605 from the center of the Sichuan Basin found that the Lower Cambrian shales achieved
606 peak oil generation during the Middle Jurassic (ca. 175 – 161 Ma) (Liu et al., 2009;
607 Zhang et al., 2005). Fluid inclusion homogenization temperatures (~120 ºC) and basin
608 modeling in the Weiyuan gas field in the southwest Sichuan Basin also indicate that oil
609 generation and migration occurred during the Triassic and Juriassic (ca. 200 – 170 Ma)
610 (Fig. 7) (Ma et al., 2007a; Tang et al., 2004; Zou et al., 2014b).
611 Integrating previous research work and the organic geochemistry, and Re-Os isotope
612 analysis results of this study, we propose that the hydrocarbon evolution in
613 Kuangshangliang area happened as follows:
614 (1) During the Early Palaeozoic, the Late Neoproterozoic Doushantuo and Early
615 Cambrian Qiongzhusi formations were buried to a depth of more than 2500 m and
616 entering the oil window (Ro ~0.80), and leading to the first phase of oil generation.
617 Following this oil generation event, the Caledonian Orogeny (~450 - 400 Ma) resulted
618 in ~2000 m of uplift and thus halted hydrocarbon maturation of the Late Neoproterozoic
619 and Early Cambrian source rocks (Fig. 7A, B).
620 (2) As a result of the collison following the Indosinian-Yanshan orogenies during the
621 Triassic and Jurassic, the Late Neoproterozoic Doushantuo and Early Cambrian
622 Qiongzhusi formations were buried to a depth of more than 5000 m (Ro ~1.2) (Fig. 7C),
623 leading to the second phase of oil generation from these formations.
624 (3) Although no meaningful Re-Os age can be obtained from the present day oil seeps,
625 the organic geochemisty data generated in this study along with the previous research
626 work indicates that this oil may have been generated during the Mesozoic from a

Permian source, i.e. the Dalong Formation (Fig. 7C).

(4) Since the Cretaceous, continued tectonics, due to the collision between the Indian and Asian plates, has caused the rapid uplift and denudation of the entire Longmen Shan Thrust Belt (Dai, 2011; Yan et al., 2011). This erosion effect has exhumed the majority of the traps and reservoirs within the the petroleum systems (Fig. 7D).

7. Implications and Conclusions

Combining the bitumen and present day oil seep organic geochemisty and Re-Os isotope geochronology from Kuangshanliang area we provide quantitative constraints on the petroleum evolution within the northern Longmen Shan Thrust Belt and adjacent basins that record a similar temporal tectonic evolution. The organic geochemisty of all the bitumen in the Kuangshanliang area from both dykes and fault/fractures possess similar characteristic and suggest they are sourced from shales of the Late Neoproterozoic to Early Cambrian Doushantuo and Qiongzhusi formations. In contrast, the few organic geochemistry of the present day oil seeps indicate the oil seeps possess distinct characteristics in comparison to the bitumen (e.g., lower tT24/TR26 (~0.5) value, higher GAM/H_{30} (3.9-7.6), DH_{30}/H_{30} (3.1-5.5) ratio and $\delta^{13}C$ (-25.9 ‰ to -27.7 ‰) and are suggestive of being derived from the Permian Dalong Formation.

The Re-Os isotope analysis showed that the Kuangshanliang area bitumen which has been derived from liquid hydrocarbon has two distinct episodes of generation. The Re-Os data for bitumen from Dyke 1 and 3 yield a date of ca. 486 Ma. This Latest Cambiran to Earliest Ordovician age agrees well with previous understanding that the Late Neoproterozoic – Early Cambrian shales of the Doushantuo and Qiongzhusi formations in the Longmen Shan Thrust Belt and adjacent Sichuan Basin first entered

into the oil window during the Ordovician based on basin burial modeling, and source rock maturation history (Liu et al., 2009; Yuan et al., 2012; Zhou et al., 2013). In contrast, the Re-Os data of bitumen from Dyke 2 and the fault/fractures yield a Middle Jurassic age (ca. 172 - 162 Ma). This Middle Jurassic age is coincident with the timing of the Indosinian-Yanshan orogenies (Arne et al., 1997; Jin et al., 2009b; Liu et al., 1996; Yan et al., 2003), which lead to the second phase of oil generation from the shales of the Late Neoproterozoic Doushantuo and Early Cambrian Qiongzhusi formations (Liu et al., 2009; Zou et al., 2014b). Additionally, the timing is in agreement with the basin modelling and the homogenization temperatures (~120 ºC) of fluid inclusions in dolomite and quartz from the adjacent Sichuan Basin showing oil generation and migration occurred between the Triassic and Juraissic (Ma et al., 2007a; Tang et al., 2004; Zou et al., 2014b).

This research shows that Re-Os isotope analyses of bitumen have the potential to record multiple oil generation episodes in complex tectonic settings. In addition to the Longmen Shan Thrust Belt and the adjacent Sichuan Basin, multiple hydrocarbon generation phases related to tectonism are also reported in the Maracaibo Basin of Venezuela (Eocene and Miocene to present two continuous oil genertion episodes) (Lugo and Mann, 1995; Talukdar et al., 1986) and the Tarim Basin of Northwest China (two phases of oil generation during the Late Silurian and Late Permian) (Xin et al., 2011). Thus, hydrocarbon (bitumen and oil) Re-Os chronology could aid in quantitatively constraining the petroleum evolution in basins worldwide, which may enhance our understanding of both the temporal and spatial evolution of a hydrocarbon system.

References

Arne, D., B. Worley, C. Wilson, S. F. Chen, D. Foster, Z. L. Luo, S. G. Liu, and P. Dirks, 1997, Differential exhumation in response to episodic thrusting along the eastern margin of the Tibetan Plateau: Tectonophysics, v. 280, p. 239-256.

Boles, J. R., P. Eichhubl, G. Garven, and J. Chen, 2004, Evolution of a hydrocarbon migration pathway along basin-bounding faults: Evidence from fault cement: AAPG bulletin, v. 88, p. 947-970.

Bordenave, M., and J. Hegre, 2005, The influence of tectonics on the entrapment of oil in the Dezful Embayment, Zagros Foldbelt, Iran: Journal of Petroleum Geology, v. 28, p. 339-368.

Burchfiel, B. C., C. Zhiliang, L. Yupinc, and L. H. Royden, 1995, Tectonics of the Longmen Shan and Adjacent Regions, Central China: International Geology Review, v. 37, p. 661-735.

Chen, S., C. J. Wilson, and B. A. Worley, 1995, Tectonic transition from the Songpan‐Garzê Fold Belt to the Sichuan Basin, south‐western China: Basin Research, v. 7, p. 235-253.

Chen, S. F., C. Wilson, Z. L. Luo, and Q. D. Deng, 1994, The evolution of the western Sichuan foreland basin, southwestern China: Journal of Southeast Asian Earth Sciences, v. 10, p. 159-168.

Chen, S. F., and C. J. Wilson, 1996, Emplacement of the Longmen Shan Thrust—Nappe Belt along the eastern margin of the Tibetan Plateau: Journal of Structural Geology, v. 18, p. 413-430.

Chen, Z., D. Jia, G. Wei, B. Li , Q. Zeng, and Q. Hu, 2005, Structural analysis of Kuangshanliang in the northern Longmenshan fold-thrust belt and its hydrocarbon exploration: Earth Science Frontiers, v. 12, p. 445-450.

Cohen, A. S., A. L. Coe, J. M. Bartlett, and C. J. Hawkesworth, 1999, Precise Re–Os ages of organic-rich mudrocks and the Os isotope composition of Jurassic seawater: Earth and Planetary Science Letters, v. 167, p. 159-173.

Cole, G. A., R. J. Drozd, R. A. Sedivy, and H. I. Halpern, 1987, Organic geochemistry and oil-source correlations, Paleozoic of Ohio: AAPG Bulletin, v. 71, p. 788-809.

Cumming, V. M., D. Selby, P. G. Lillis, and M. D. Lewan, 2014, Re–Os geochronology and Os isotope fingerprinting of petroleum sourced from a Type I lacustrine kerogen: Insights from the natural Green River petroleum system in the Uinta Basin and hydrous pyrolysis experiments: Geochimica et Cosmochimica Acta, v. 138, p. 32-56.

Dai, H., S. Liu, W. Sun, K. Han, Z. Luo, Z. Xie, and Y. Huang, 2009, Study on characteristics of Sinian-Silurian bitumen outcrops in the Longmenshan-Micangshan area, Southwest China: Journal of Chengdu University of Technology (Science & Technology Edition), v. 36, p. 687-696.

Dai, J., 2011, Analysis on Strcutural Deformation Stages and Dynamic Genesis of Thrust Belt in Longmen Mountain: Journal of Southwest Petroleum University, v. 33, p. 61-67.

De Grande, S., F. A. Neto, and M. Mello, 1993, Extended tricyclic terpanes in sediments and petroleums: Organic geochemistry, v. 20, p. 1039-1047.

720 Deng, B., S. Liu, L. Jansa, J. Cao, Y. Cheng, Z. Li, and S. Liu, 2012, Sedimentary
721 record of Late Triassic transpressional tectonics of the Longmenshan thrust belt,
722 SW China: Journal of Asian Earth Sciences, v. 48, p. 43-55.
723 Didyk, B., 1978, Organic geochemical indicators of palaeoenvnonmental conditions of
724 sedimentation: Nature, v. 272, p. 16.
725 Dirks, P., C. Wilson, S. Chen, Z. Luo, and S. Liu, 1994, Tectonic evolution of the NE
726 margin of the Tibetan Plateau; evidence from the central Longmen Mountains,
727 Sichuan Province, China: Journal of Southeast Asian Earth Sciences, v. 9, p.
728 181-192.
729 Esser, B. K., and K. K. Turekian, 1993, The Osmium Isotopic Composition of the
730 Continental-Crust: Geochimica Et Cosmochimica Acta, v. 57, p. 3093-3104.
731 Fall, A., P. Eichhubl, R. J. Bodnar, S. E. Laubach, and J. S. Davis, 2015, Natural
732 hydraulic fracturing of tight-gas sandstone reservoirs, Piceance Basin, Colorado:
733 Geological Society of America Bulletin, v. 127, p. 61-75.
734 Feng, C., Q. Chen, C. Tan, X. Qin, P. Zhang, and W. Meng, 2014, The stress state of the
735 Beichuan-Jiangyou segment of the Longmenshan fault before and after the
736 Wenchuan M S 8.0 Earthquake: Journal of Earth Science, v. 25, p. 861-870.
737 Finlay, A. J., D. Selby, and M. J. Osborne, 2011, Re-Os geochronology and
738 fingerprinting of United Kingdom Atlantic margin oil: Temporal implications
739 for regional petroleum systems: Geology, v. 39, p. 475-478.
740 Finlay, A. J., D. Selby, and M. J. Osborne, 2012, Petroleum source rock identification of
741 United Kingdom Atlantic Margin oil fields and the Western Canadian Oil Sands
742 using Platinum, Palladium, Osmium and Rhenium: Implications for global
743 petroleum systems: Earth and Planetary Science Letters, v. 313, p. 95-104.
744 Ge, X., C. Shen, D. Selby, D. Deng, and L. Mei, 2016, Apatite fission-track and Re-Os
745 geochronology of the Xuefeng uplift, China: Temporal implications for dry gas
746 associated hydrocarbon systems: Geology, v. 44, p. 491-494.
747 Georgiev, S. V., H. J. Stein, J. L. Hannah, R. Galimberti, M. Nali, G. Yang, and A.
748 Zimmerman, 2016, Re–Os dating of maltenes and asphaltenes within single
749 samples of crude oil: Geochimica et Cosmochimica Acta, v. 179, p. 53-75.
750 Gramlich, J. W., T. J. Murphy, E. L. Garner, and W. R. Shields, 1973, Absolute Isotopic
751 Abundance Ratio and Atomic Weight of a Reference Sample of Rhenium:
752 Journal of reserch of the Notional Bureau of Standards - A. Physics and
753 Chemistry, v. 77A, p. 691-698.
754 Hackley, P. C., R. T. Ryder, M. H. Trippi, and H. Alimi, 2013, Thermal maturity of
755 northern Appalachian Basin Devonian shales: insights from sterane and terpane
756 biomarkers: Fuel, v. 106, p. 455-462.
757 Harrowfield, M. J., and C. J. Wilson, 2005, Indosinian deformation of the Songpan
758 Garze fold belt, northeast Tibetan Plateau: Journal of Structural Geology, v. 27,
759 p. 101-117.
760 Huang, D., and L. Wang, 2008, Geochemical characteristics of bituminous dike in
761 Kuangshanliang area of the Northwestern Sichuan Basin and its significance:
762 Acta Petrolei Sinica, v. 29, p. 23-28.
763 Huang, M., R. Maas, I. Buick, and I. Williams, 2003, Crustal response to continental
764 collisions between the Tibet, Indian, South China and North China blocks:
765 Geochronological constraints from the Songpan - Garze orogenic belt, western
766 China: Journal of Metamorphic Geology, v. 21, p. 223-240.

767 Huang, W., S. Liu, G. Xu, G. Wang, W. Ma, C. Zhang, and G. Song, 2011,
768 Characteristics of paleo oil pools from Sinian to Lower Paleozoic in
769 southeastern margin of Sichuan Basin: Geological Review, v. 57, p. 285-299.
770 Hwang, R., S. Teerman, and R. Carlson, 1998, Geochemical comparison of reservoir
771 solid bitumens with diverse origins: Organic Geochemistry, v. 29, p. 505-517.
772 Jia, D., G. Wei, Z. Chen, B. Li, Q. Zeng, and G. Yang, 2006, Longmen Shan fold-thrust
773 belt and its relation to the western Sichuan Basin in central China: New insights
774 from hydrocarbon exploration: AAPG Bulletin, v. 90, p. 1425-1447.
775 Jiang, S.-Y., J.-H. Yang, H.-F. Ling, Y.-Q. Chen, H.-Z. Feng, K.-D. Zhao, and P. Ni,
776 2007, Extreme enrichment of polymetallic Ni–Mo–PGE–Au in Lower Cambrian
777 black shales of South China: An Os isotope and PGE geochemical investigation:
778 Palaeogeography, Palaeoclimatology, Palaeoecology, v. 254, p. 217-228.
779 Jin, W., L. Tang, K. Yang, G. Wan, and Z. Lü, 2010, Segmentation of the Longmen
780 Mountains thrust belt, western Sichuan foreland basin, SW China:
781 Tectonophysics, v. 485, p. 107-121.
782 Jin, W., L. Tang, K. Yang, G. Wan, Z. Lü, and Y. Yu, 2009a, Transfer zones within the
783 Longmen Mountains thrust belt, SW China: Geosciences Journal, v. 13, p. 1-14.
784 Jin, W., L. Tang, K. Yang, G. Wan, and Z. Lu, 2008, Progress and problem of study on
785 characters of the Longmen Mountain thrust belt: Geological Review, v. 54, p.
786 37-46.
787 Jin, W., L. Tang, K. Yang, G. Wan, Z. Lv, and Y. Yu, 2009b, Tectonic evolution of the
788 middle frontal area of the Longmen Mountain thrust belt, western Sichuan basin,
789 China: Acta Geologica Sinica (English Edition), v. 83, p. 92-102.
790 Kendall, B., R. A. Creaser, and D. Selby, 2009, 187Re-187Os geochronology of
791 Precambrian organic-rich sedimentary rocks: Geological Society, London,
792 Special Publications, v. 326, p. 85-107.
793 Lei, Y., C. Jia, B. Li , G. Wei, Z. Chen, and X. Shi, 2012, Meso‐Cenozoic Tectonic
794 Events Recorded by Apatite Fission Track in the Northern Longmen‐Micang
795 Mountains Region: Acta Geologica Sinica (English edition), v. 86, p. 153-165.
796 Li, C., L. Wen, and S. Tao, 2015, Characteristics and enrichment factors of supergiant
797 Lower Cambrian Longwangmiao gas reservoir in Anyue gas field: the oldest and
798 largest single monoblock gas reservoir in China: Energy, Exploration &
799 Exploitation, v. 33, p. 827-850.
800 Li, J., Z. Li, and P. Wang, 2012, The preliminary analysis of structure pattern of
801 Longmeshan tectonic zone of Sichuan: Yunnan Geology, v. 31, p. 272-276.
802 Li, J., Z. Wang, and M. Zhao, 1999, 40Ar/39Ar Thermochronological Constraints on
803 the Timing of Collisional Orogeny in the Mian‐Lüe Collision Belt, Southern
804 Qinling Mountains: Acta Geologica Sinica (English edition), v. 73, p. 208-215.
805 Li, X., Z. Wang, X. Zhang, Q. Liu, and J. Yan, 2001, Charactersitics of Paleo-Uplifts in
806 Sichuan Basin and their control on natural gases: Oil & Gas Geology, v. 22, p.
807 347-351.
808 Li, Z., S. Liu, H. Chen, S. Liu, B. Guo, and X. Tian, 2008, Structural segmentation and
809 zonation and differential deformation across and along the Lomgmen thrust belt,
810 West Sichuan: Journal of Chengdu University of Technology (Science &
811 Technology Edition), v. 35, p. 440-455.
812 Liang, D., 2007, Evaluation on Efficient Source Rock of Complex Structure Area in
813 Southern China, The China Petroleum & Chemical Corporation.

814 Lillis, P. G., and D. Selby, 2013, Evaluation of the rhenium–osmium geochronometer in
815 the Phosphoria petroleum system, Bighorn Basin of Wyoming and Montana,
816 USA: Geochimica et Cosmochimica Acta, v. 118, p. 312-330.
817 Lin, J., Y. Xie, J. Liu, Z. Zhao, X. Jing, and H. Cheng, 2011, Restudy of the source rock
818 of Majiang paleo-reservoir: Geological Science and Technology Information, v.
819 30, p. 105-109.
820 Liu, G., S. Wang, W. Pan, and J. Lv, 2003, Characteristics of Tianjingshan destroyed oil
821 reservoir in Guangyuan Area, Sichuan: Marine Origin Petroleum Geology, v. 8,
822 p. 103-108.
823 Liu, Q., D. Zhu, Z. Jin, C. Liu, D. Zhang, and Z. He, 2016, Coupled alteration of
824 hydrothermal fluids and thermal sulfate reduction (TSR) in ancient dolomite
825 reservoirs–An example from Sinian Dengying Formation in Sichuan Basin,
826 southern China: Precambrian Research, v. 285, p. 39-57.
827 Liu, S., B. Deng, Z. Li, and W. Sun, 2011, The texture of sedimentary basin-orogeny
828 belt system and its influence on oil/gas distribution: A case study from Sichuan
829 basin: Acta Petrologica Sinica, v. 27, p. 621-635.
830 Liu, S., Z. Luo, S. Dai, D. Arne, and C. Wilson, 1996, The uplift of the Longmenshan
831 thrust belt and subsidence of the west Sichuan Foreland Basin: Acta Geologica
832 Sinica (English Edition), v. 9, p. 16-26.
833 Liu, S., Y. Ma, X. Cai, G. Xu, G. Wang, Z. Yong, W. Sun, H. Yuan, and C. Pan, 2009,
834 Characteristic and accumulation process of the natural gas from Sinian to Lower
835 Paleozoic in Sichuan Basin: China. Journal of Chengdu University of
836 Technology (Science & Technology Edition), v. 33, p. 345-354.
837 Liu, S., R. Steel, and G. Zhang, 2005, Mesozoic sedimentary basin development and
838 tectonic implication, northern Yangtze Block, eastern China: record of
839 continent–continent collision: Journal of Asian Earth Sciences, v. 25, p. 9-27.
840 Liu, S., X. Zhao, Z. Luo, G. Xu, and G. Wang, 2001, Study on the tectonic events in the
841 system of the Longmen Mountain-west Sichuan foreland basin, China: Journal
842 of Chengdu University of Technology, v. 28, p. 221-230.
843 Ludwig, K., 2003, A plotting and regression program for radiogenic-isotope data,
844 version 3.00: United State Geol Survey, open file report, p. 1-70.
845 Lugo, J., and P. Mann, 1995, Jurassic-Eocene tectonic evolution of Maracaibo basin,
846 Venezuela: AAPG Special Volumes, p. 699-725.
847 Ma, Y., X. Cai, and T. Guo, 2007a, The controlling factors of oil and gas charging and
848 accumulation of Puguang gas field in the Sichuan Basin: Chinese Science
849 Bulletin, v. 52, p. 193-200.
850 Ma, Y., X. Cai, P. Zhao, Y. Luo, and X. Zhang, 2010, Distribution and futher
851 exploration of the Large-medium sized gas field in Sichuan Basin: Acta
852 Geologica Sinica, v. 31, p. 347-354.
853 Ma, Y., X. Guo, T. Guo, R. Huang, X. Cai, and G. Li, 2007b, The Puguang gas field:
854 New giant discovery in the mature Sichuan Basin, southwest China: AAPG
855 bulletin, v. 91, p. 627-643.
856 Moretti, I., P. Baby, E. Mendez, and D. Zubieta, 1996, Hydrocarbon generation in
857 relation to thrusting in the Sub Andean zone from 18 to 22 degrees S, Bolivia:
858 Petroleum Geoscience, v. 2, p. 17-28.
859 Nowell, G., D. Pearson, S. Parman, A. Luguet, and E. Hanski, 2008, Precise and
860 accurate 186 Os/188 Os and 187 Os/188 Os measurements by multi-collector
861 plasma ionisation mass spectrometry, part II: Laser ablation and its application

862 to single-grain Pt–Os and Re–Os geochronology: Chemical Geology, v. 248, p.
863 394-426.
864 Parnell, J., and I. Swainbank, 1990, Pb-Pb dating of hydrocarbon migration into a
865 bitumen-bearing ore deposit, North Wales: Geology, v. 18, p. 1028-1030.
866 Peters, K., C. Walters, and J. Moldowan, 2005, The Biomarker guide, biomarkers and
867 isotopes in petroleum exploration and earth history, vol 1–2, Cambridge
868 University Press, New York, 961 p.
869 Peters, K. E., and J. M. Moldowan, 1993, The biomarker guide: interpreting molecular
870 fossils in petroleum and ancient sediments: United States, Englewood Cliffs, NJ
871 (United States); Prentice Hall.
872 Pusey, W. C., 1973, How to evaluate potential gas and oil source rocks: World Oil, v.
873 176, p. 71-75.
874 Rao, D., J. Qin, Tenger, and M. Zhang, 2008, Source analysis of oil seepage and
875 bitumen originating from marine layer strata in Guangyuan area, the northwest
876 Sichuan Basin: Petroleum Geology & Experiment, v. 30, p. 596-599.
877 Ravizza, G., and K. Turekian, 1992, The osmium isotopic composition of organic-rich
878 marine sediments: Earth and Planetary Science Letters, v. 110, p. 1-6.
879 Rooney, A., 2011, Re-Os geochronology and geochemistry of Proterozoic sedimentary
880 successions, Durham University, Durham, 114 p.
881 Rooney, A. D., D. Selby, J.-P. Houzay, and P. R. Renne, 2010, Re–Os geochronology
882 of a Mesoproterozoic sedimentary succession, Taoudeni basin, Mauritania:
883 implications for basin-wide correlations and Re–Os organic-rich sediments
884 systematics: Earth and Planetary Science Letters, v. 289, p. 486-496.
885 Seifert, W., and J. Moldowan, 1986, Use of biological markers in petroleum
886 exploration: Methods in geochemistry and geophysics, v. 24, p. 261-290.
887 Selby, D., and R. A. Creaser, 2005, Direct radiometric dating of hydrocarbon deposits
888 using rhenium-osmium isotopes: Science, v. 308, p. 1293-1295.
889 Selby, D., R. A. Creaser, K. Dewing, and M. Fowler, 2005, Evaluation of bitumen as a
890 187 Re–187 Os geochronometer for hydrocarbon maturation and migration: A
891 test case from the Polaris MVT deposit, Canada: Earth and Planetary Science
892 Letters, v. 235, p. 1-15.
893 Selby, D., R. A. Creaser, and M. G. Fowler, 2007, Re–Os elemental and isotopic
894 systematics in crude oils: Geochimica et Cosmochimica Acta, v. 71, p. 378-386.
895 Smoliar, M. I., R. J. Walker, and J. W. Morgan, 1996, Re-Os ages of group IIA, IIIA,
896 IVA, and IVB iron meteorites: Science, v. 271, p. 1099-1102.
897 Summons, R. E., J. M. Hope, R. Swart, and M. R. Walter, 2008, Origin of Nama Basin
898 bitumen seeps: Petroleum derived from a Permian lacustrine source rock
899 traversing southwestern Gondwana: Organic Geochemistry, v. 39, p. 589-607.
900 Sun, D., 2011, The structural character and Meso-Cenozoic evolution of Micang
901 Mountain structural zone, Northern Sichuan basin, China, Chengdu University
902 of Technology, Chengdu, 206 p.
903 Sun, W., S. Liu, K. Han, Z. Luo, G. Wang, and G. Xu, 2009, The Petroleum Geological
904 Condition and Exploration Prospect Analysis in Sinian, Sichuan Basin:
905 Petroleum Geology & Experiment, v. 31, p. 350-355.
906 Talukdar, S., O. Gallango, and M. Chin-A-Lien, 1986, Generation and migration of
907 hydrocarbons in the Maracaibo Basin, Venezuela: An integrated basin study:
908 Organic Geochemistry, v. 10, p. 261-279.

909 Tang, J., T. Zhang, Z. Bao, and M. Zhang, 2004, Study of Organic Inclusion in the
910 Carbonate Reservoir Bed of the Weiyuan Gas Field in the Sichuan Basin:
911 Geological Review, v. 50, p. 210-214.
912 Tian, X., 2009, Structural Features in the northern segment of Longmen Mountains and
913 the discussion on its hydrocarbon prospects, Chengdu University of Technology,
914 Chengdu, 91 p.
915 Tissot, B. P., and D. H. Welte, 1984, Petroleum formation and occurrence: Other
916 Information: From review by Edward A. Beaumont, in The American
917 Association of Petroleum Geologists Bulletin, Vol. 71, No. 4 (April 1987),
918 Medium: X; Size: Pages: 699 p.
919 Urien, C. M., J. Zambrano, and M. Yrigoyen, 1995, Petroleum basins of southern South
920 America: an overview: AAPG Bulletin, v. special, p. 63-77.
921 Wang, L., K. Han, B. Xie, J. Zhang, M. Du, M. Wan, and D. Li, 2005, Reservoiring
922 conditions of the oil and gas fields in the North section of Longmen Mountain
923 Nappe structural belts: Natural Gas Industry, v. 25, p. 1-5.
924 Wang, M., C. Bao, and M. Xiao, 1989, Peroleum Geology of China (Vol. 10) Sichuan
925 Oil & Gas Field v. 10, Petroleum Idustry Press (Beijing), 516 p.
926 Wang, S., and X. Li, 1999, Geochemistry of the Sinian natural gases and petroleum
927 systems in the Weiyuan–Ziyan area: Natural Gas Geosciences Journal, v. 10, p.
928 63-69.
929 Wang, S., B. Zheng, and L. Cai, 1997, The Destroyed Oil Pools in South China and
930 Hydrocarbon Prospecting: Marine Origin Petroleum Geology, v. 2, p. 44-50.
931 Wang, Y., W. Fan, G. Zhao, S. Ji, and T. Peng, 2007, Zircon U–Pb geochronology of
932 gneissic rocks in the Yunkai massif and its implications on the Caledonian event
933 in the South China Block: Gondwana Research, v. 12, p. 404-416.
934 Wang, Y., S. Liu, B. Fu, and S. Xing, 2015, Quantitative estimation of surface
935 denudation in Longmen Shan during late cenozoic: Earth Science - Journal of
936 China University of Geosciences, v. 40, p. 953-964.
937 Wei, G., G. Chen, S. Du, L. Zhang, and W. Yang, 2008, Petroleum systems of the oldest
938 gas field in China: Neoproterozoic gas pools in the Weiyuan gas field, Sichuan
939 Basin: Marine and Petroleum Geology, v. 25, p. 371-386.
940 Wenger, L. M., and G. H. Isaksen, 2002, Control of hydrocarbon seepage intensity on
941 level of biodegradation in sea bottom sediments: Organic Geochemistry, v. 33,
942 p. 1277-1292.
943 Wilson, C. J., M. J. Harrowfield, and A. J. Reid, 2006, Brittle modification of Triassic
944 architecture in eastern Tibet: implications for the construction of the Cenozoic
945 plateau: Journal of Asian Earth Sciences, v. 27, p. 341-357.
946 Worley, B. A., and C. J. Wilson, 1996, Deformation partitioning and foliation
947 reactivation during transpressional orogenesis, an example from the Central
948 Longmen Shan, China: Journal of Structural Geology, v. 18, p. 395-411.
949 Wu, L., Y. Liao, Y. Fang, and A. Geng, 2012, The study on the source of the oil seeps
950 and bitumens in the Tianjingshan structure of the northern Longmen Mountain
951 structure of Sichuan Basin, China: Marine and Petroleum Geology, v. 37, p.
952 147-161.
953 Xie, B., L. Wang, J. Zhang, and S. Chen, 2003, Vertical Distribution and Geochemical
954 Behaviours of the Hydrocarbon Source Rocks in the North Section of Longmen
955 Mountains: Natural Gas Industry, v. 23, p. 21-24.

956 Xin, Y., N. Qiu, J. Qin, and L. Zheng, 2011, Study on Second Hydrocarbon Generation
957 of Ordovician Hydrocarbon Source Rock in Tarim Basin: Journal of Earth
958 Science and Environment, v. 33, p. 261-267.
959 Xu, G., J. L. Hannah, H. J. Stein, B. Bingen, G. Yang, A. Zimmerman, W. Weitschat,
960 A. Mørk, and H. M. Weiss, 2009, Re–Os geochronology of Arctic black shales
961 to evaluate the Anisian–Ladinian boundary and global faunal correlations: Earth
962 and Planetary Science Letters, v. 288, p. 581-587.
963 Xu, G., J. L. Hannah, H. J. Stein, A. Mørk, J. O. Vigran, B. Bingen, D. L. Schutt, and B.
964 A. Lundschien, 2014, Cause of Upper Triassic climate crisis revealed by Re–Os
965 geochemistry of Boreal black shales: Palaeogeography, Palaeoclimatology,
966 Palaeoecology, v. 395, p. 222-232.
967 Yahi, N., R. G. Schaefer, and R. Littke, 2001, Petroleum generation and accumulation
968 in the Berkine basin, eastern Algeria: AAPG bulletin, v. 85, p. 1439-1467.
969 Yan, D., M. Zhou, S. Li, and G. Wei, 2011, Structural and geochronological constraints
970 on the Mesozoic-Cenozoic tectonic evolution of the Longmen Shan thrust belt,
971 eastern Tibetan Plateau: Tectonics, v. 30, p. 1-24.
972 Yan, D., M. Zhou, H. Song, X. Wang, and J. Malpas, 2003, Origin and tectonic
973 significance of a Mesozoic multi-layer over-thrust system within the Yangtze
974 Block (South China): Tectonophysics, v. 361, p. 239-254.
975 Yang, C., Z. Wang, B. P. Hollebone, C. E. Brown, and M. Landriault, 2009,
976 Characteristics of bicyclic sesquiterpanes in crude oils and petroleum products:
977 Journal of Chromatography A, v. 1216, p. 4475-4484.
978 Yuan, H., J. Liang, D. Gong, G. Xu, S. Liu, and G. Wang, 2012, Formation and
979 evolution of Sinian oil and gas pools in typical structures, Sichuan Basin, China:
980 Petroleum Science, v. 9, p. 129-140.
981 Zhang, L., G. Wei, S. Wu, Z. Wang, X. Xiao, P. Zhang, and Y. Shen, 2005, Distribution
982 Characters and Hydrocarbon-Generating Potential of Bitumen of Sinian-Lower
983 Palaeozoic in Sichuan Basin: Petroleum Geology and Experiment v. 27, p. 276-
984 280.
985 Zhang, S., A. Hanson, J. Moldowan, S. Graham, D. Liang, E. Chang, and F. Fago, 2000,
986 Paleozoic oil–source rock correlations in the Tarim basin, NW China: Organic
987 Geochemistry, v. 31, p. 273-286.
988 Zhang, S., and G. Zhu, 2006, Gas accumulation characteristics and exploration potential
989 of marine sediments in Sichuan Basin: Acta Petrolei Sinica, v. 27, p. 1-8.
990 Zhou, Q., X. Xiao, H. Tian, and R. Wilkins, 2013, Oil charge history of bitumens of
991 differing maturities in exhumed Palaeozoic reservoir rocks at Tianjingshan, NW
992 Sichuan Basin, southern China: Journal of Petroleum Geology, v. 36, p. 363-
993 382.
994 Zhu, B., J. Zhang, X. Tu, X. Chang, C. Fan, Y. Liu, and J. Liu, 2001, Pb, Sr, and Nd
995 isotopic features in organic matter from China and their implications for
996 petroleum generation and migration: Geochimica et Cosmochimica Acta, v. 65,
997 p. 2555-2570.
998 Zhuang, G., 1985, Regional geology of Guangxi Zhuang Autonomous Region,
999 Geological Publishing House, 853 p.
1000 Zou, C., J. Du, C. Xu, Z. Wang, B. Zhang, G. Wei, T. Wang, G. Yao, S. Deng, and J.
1001 Liu, 2014a, Formation, distribution, resource potential, and discovery of Sinian–
1002 Cambrian giant gas field, Sichuan Basin, SW China: Petroleum Exploration and
1003 Development, v. 41, p. 306-325.

Zou, C., G. Wei, C. Xu, J. Du, Z. Xie, Z. Wang, L. Hou, C. Yang, J. Li, and W. Yang, 2014b, Geochemistry of the Sinian–Cambrian gas system in the Sichuan Basin, China: Organic Geochemistry, v. 74, p. 13-21.
Zumberge, J. E., 1987, Prediction of source rock characteristics based on terpane biomarkers in crude oils: A multivariate statistical approach: Geochimica et Cosmochimica Acta, v. 51, p. 1625-1637.

Author's vita

Xiang Ge

Key Laboratory of Tectonics and Petroleum Resources (China University of Geosciences), Ministry of Education, Wuhan, 430074, China; 388 Lumo Road, Hongshan District, Wuhan City, Hubei Province, China.

Department of Earth Sciences, Durham University, Durham, DH1 3LE, UK; Arthur Holmes Building, Science Site, South Road, Durham, England, UK

xiangge89@126.com

Xiang Ge is a Joint Ph.D student at the China University of Geoscience (Wuhan) and Durham University. He received his B.Sc. and M.Sc. from China University of Geoscience (Wuhan). His PhD thesis is focusing on the petroleum geology of the Sichuan Basin applying hydrocarbon Re-Os isotope, structural and tectonic analyses.

Chuanbo Shen (*Corresponding author)

Key Laboratory of Tectonics and Petroleum Resources (China University of Geosciences), Ministry of Education, Wuhan, 430074, China; 388 Lumo Road, Hongshan District, Wuhan City, Hubei Province, China.

cugshen@126.com

Chuanbo Shen is currently a professor in the Faculty of Earth Resources at the China University of Geosciences (Wuhan). He received his B.Sc., M.Sc., and Ph.D. from

China University of Geoscience (Wuhan). He also completed postdoctoral research in Technische Universität Bergakademie Freiberg, Germany. His present research interests are low-temperature thermochronology, tectonic-thermal evolution and hydrocarbon geochronology.

David Selby

Department of Earth Sciences, Durham University, Durham, DH1 3LE, UK

david.selby@durham.ac.uk

David Selby is a Professor of Earth Sciences at Durham University, UK. He received a bachelor's degree in geology from Southampton University, UK and Ph.D. degree from the University of Alberta, Canada. He also carried out his postdoctoral research at the University of Alberta. His research focuses on the Earth Science disciplines of economic geology, petroleum geoscience and paleoclimate / oceanography, principally through the application and development of the novel, state-of-the-art, rhenium-osmium radio isotope methodology.

Jie Wang

Wuxi institute of petroleum geology, SINOPEC, Wuxi, 214151, China

wangjie.syky@sinopec.com

Jie Wang is now a Senior Engineer in Wuxi institute of petroleum geology, SINOPEC. He obtained his B.Sc. degree in Petroleum Engineering from Xi'an Shiyou University and M.Sc. and Ph.D. degree from Lanzhou Geological Institute, Chinese Academy of Sciences. He also carried out his postdoctoral research at the Zhejiang University and Wuxi institute of petroleum geology in 2005-2008. His current research focuses on

petroleum geology and organic geochemistry.

Liangbang Ma

Wuxi institute of petroleum geology, SINOPEC, Wuxi, 214151, China

malb.syky@sinopec.com

Liangbang Ma is a Senior Engineer in Wuxi institute of petroleum geology, SINOPEC. He received his B.Sc. and M.Sc. in Analytical Chemistry from Chengdu University of Technology. His current research focuses on organic geochemistry.

Xiaoyan Ruan

Key Laboratory of Tectonics and Petroleum Resources (China University of Geosciences), Ministry of Education, Wuhan, 430074, China; 388 Lumo Road, Hongshan District, Wuhan City, Hubei Province, China.

ruan6231@163.com

Xiaoyan Ruan is an Associate Professor in the Faculty of Earth Resources at the China University of Geosciences (Wuhan). She received her B.Sc., M.Sc., and Ph.D. from China University of Geosciences (Wuhan). She carried out research at Bryant University, in the United States as a visiting scholar in 2010-2011. Her current research focuses on biological geochemistry and petroleum geochemistry.

Shouzhi Hu

Key Laboratory of Tectonics and Petroleum Resources (China University of Geosciences), Ministry of Education, Wuhan, 430074, China; 388 Lumo Road, Hongshan District, Wuhan City, Hubei Province, China.

hushzh@cug.edu.cn

Shouzhi Hu is an Associate Professor in the Faculty of Earth Resources at the China University of Geosciences (Wuhan). She received her B.Sc., M.Sc., and Ph.D. in Petroleum Geology from Southwest Petroleum University. She also completed a year research in GFZ Department, Germany as a visiting scholar in 2012-2013. Her current research focuses on the petroleum geology and organic geochemistry.

Lianfu Mei

Key Laboratory of Tectonics and Petroleum Resources (China University of Geosciences), Ministry of Education, Wuhan, 430074, China; 388 Lumo Road, Hongshan District, Wuhan City, Hubei Province, China.

lfmei@cug.edu.cn

Lianfu Mei is a Professor in the Faculty of Earth Resources at the China University of Geosciences (Wuhan). He received a bachelor's degree in Mineral Prospecting and Exploration from Zhongnan University, China UK and M.Sc., and Ph.D. degree in petroleum geology from the China University of Geosciences (Wuhan). His research focuses on the structural geology and petroleum geoscience within petroliferous basins.

Figure Captions

Fig. 1. A) Regional map of the Longmen Shan Thrust Belt and the adjacent Sichuan Basin and Songpan-Garze Belt in the SE and NW, respectively. The shaded area is expanded in Figure 1B and 1C; B) Simplified map of the Sichuan Basin showing the distribution of gas fields with different orogenic belts. Substantially modified after Li et

al., 2015; Li et al., 2001; Ma et al., 2010; C) Structural map of the Longmen Shan Thrust Belt showing the bitumen outcrop distribution, and the location of the Cambrian cored Kuangshanliang anticline (our study area). Substantially modified after Tian, 2009.

Fig. 2. Stratigraphy, hydrocarbon system and tectonic events in the North Longmen Shan area. Substantially modified after Chen and Wilson, 1996; Wu et al., 2012.

Fig. 3. A) Simplified geological map of the Kuangshanliang anticline; B) Detailed geology feature in the Kuangshanliang area and locations of the bitumen and present day oil seep samples.

Fig. 4. Bitumen and oil sample locations and field relationships. A) Bitumen Dyke 1 showing the relationship between the dyke and the country rock. A') detailed image of the breccia zone shown in A. B) Bitumen sample (11SKD-3d, 11SKD-4d, 11SKD-5d, SKD-1f) locations in Dyke 1 and related fault/fractures. C) Bitumen sample (XKD-1d, XKD-2d) locations in Dyke 2. D) Syn / post thrust fault in Dyke 2. E) Bitumen sample (HSCD-1d and GY1d-6d) locations in Dyke 3. F) Bitumen samples (LXB-1f, LXB-2f) from a fault zone. G) Bitumen sample (11LXB-1f) from a fault plane. H) Present day oil seep samples (Oil-3, Oil-5, Oil-7) occurring in the Early Cambrian Qiongzhusi Formation.

Fig. 5. Total Iron Chromatogram (TIC), m/z 191 and m/z 217 mass chromatograms of the bitumen (11SKD-4d, XKD-1d, GY-3d, HSCD-1d, LXB-1f) and the present day oil seeps (Oil-5) in the Kuangshangliang area.

Fig. 6. A) Traditional $^{187}Re/^{188}Os$ vs $^{187}Os/^{188}Os$ plot showing all the Re-Os data for bitumen from the dykes and faults/fractures, as well as the present day oil seeps in the Kuangshanliang anticline (Bold for Dyke 1 bitumen; Underline for Dyke 2 bitumen; Italic for Dyke 3 bitumen; Regular font for fault/fracture bitumen and Bold Italic for the present day oil seeps). B) The Re-Os isotope data of Dyke 3 bitumen. C) The Re-Os isotope data of bitumen from Dyke 1 and 3 and fault bitumen sample, 11LXB-1f. D) The Re-Os isotope data of Dyke 1 and 3 bitumen (without HSCD-1 and GY-1). E. The Re-Os isotope data of all Dyke 2 and fault/fracture bitumen. F) The Re-Os isotope data of Dyke 2 and fault/fracture bitumen based on Os_i values groups (~1.82 and ~1.89). Data-point ellipses are shown with 2-sigma absolute uncertainty. Data labels are sample numbers listed in Table 2.

Fig. 7. The relationship between petroleum generation and tectonism. Shown is a comparison of the Re-Os ages with source rocks (Xie et al., 2003; Zhou et al., 2013), published basin model and fluid inclusion results (Ma et al., 2007a; Tang et al., 2004) and muscovite $^{40}Ar/^{39}Ar$ ages (Li et al., 1999; Yan et al., 2011), Jurassic zircon fission track ages (Arne et al., 1997) in Longmen Shan Thrust Belt. The schematic cartoon model shows the hydrocarbon evolution in the Kuangshanliang anticline, Northern Longmen Shan Thrust Belt. A) First phase of oil generation during the Ordovician, before the Caledonian Orogeny. B) Oil generation ceased due to uplift caused by the

Caledonian Orogeny (ca. 450 - 400 Ma). C) Second phase of oil generation during the Middle Jurassic Indosinian-Yanshan orogenies. D) Present condition of the bitumen and present day oil seeps after Cenozoic Himalayan Orogeny.

Figure 1

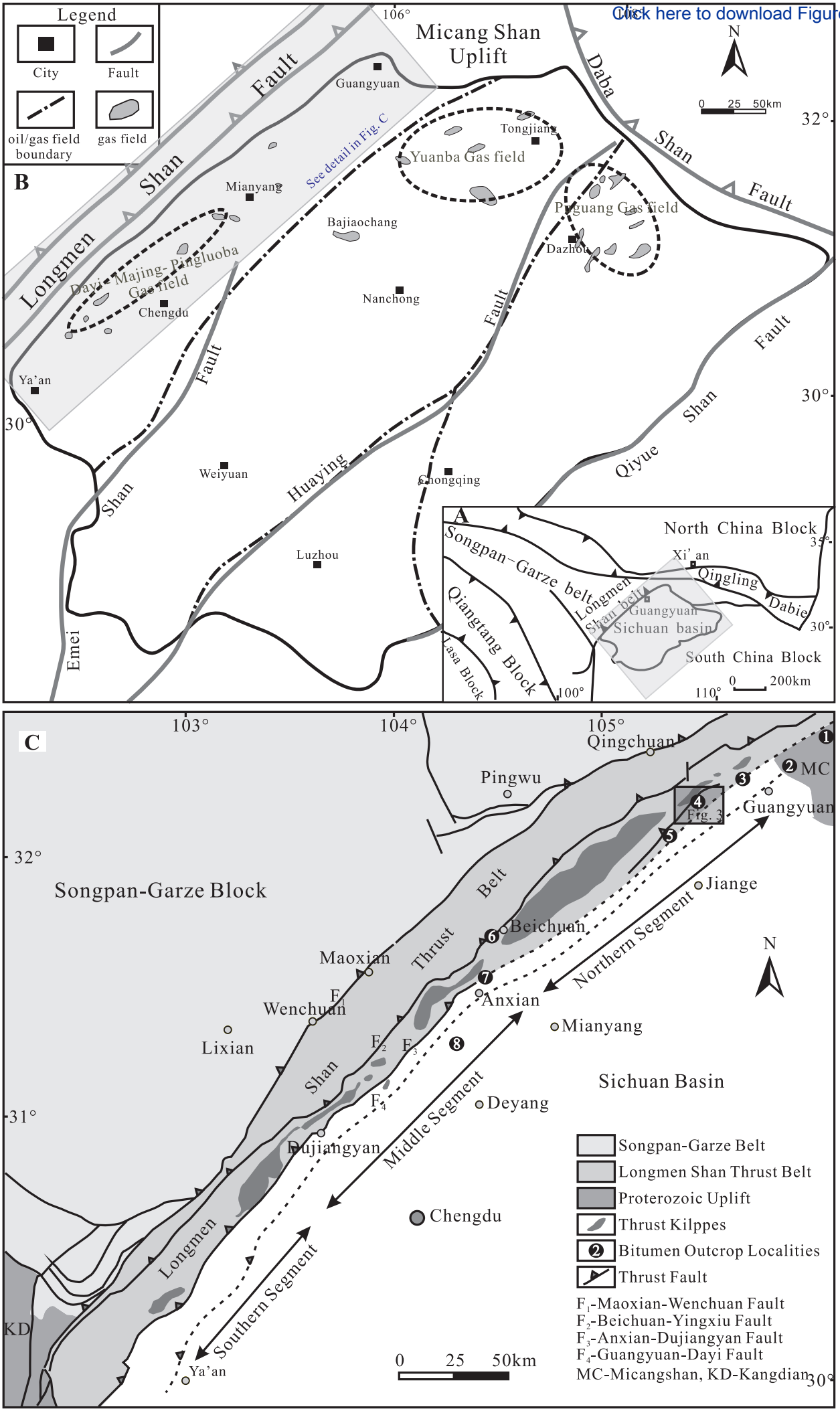

Figure 2

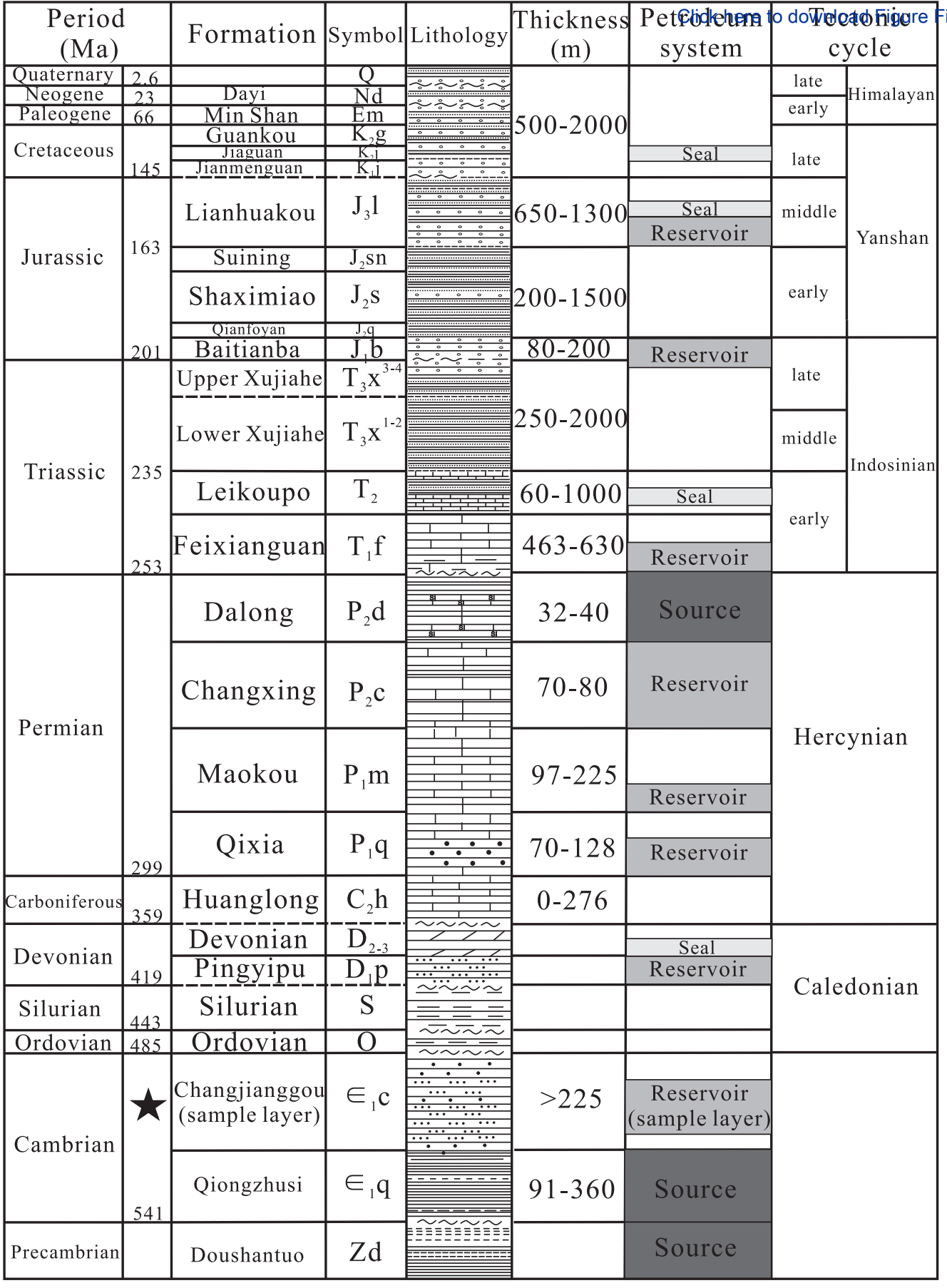

Figure 3

Click here to download Figure Fig.3.eps

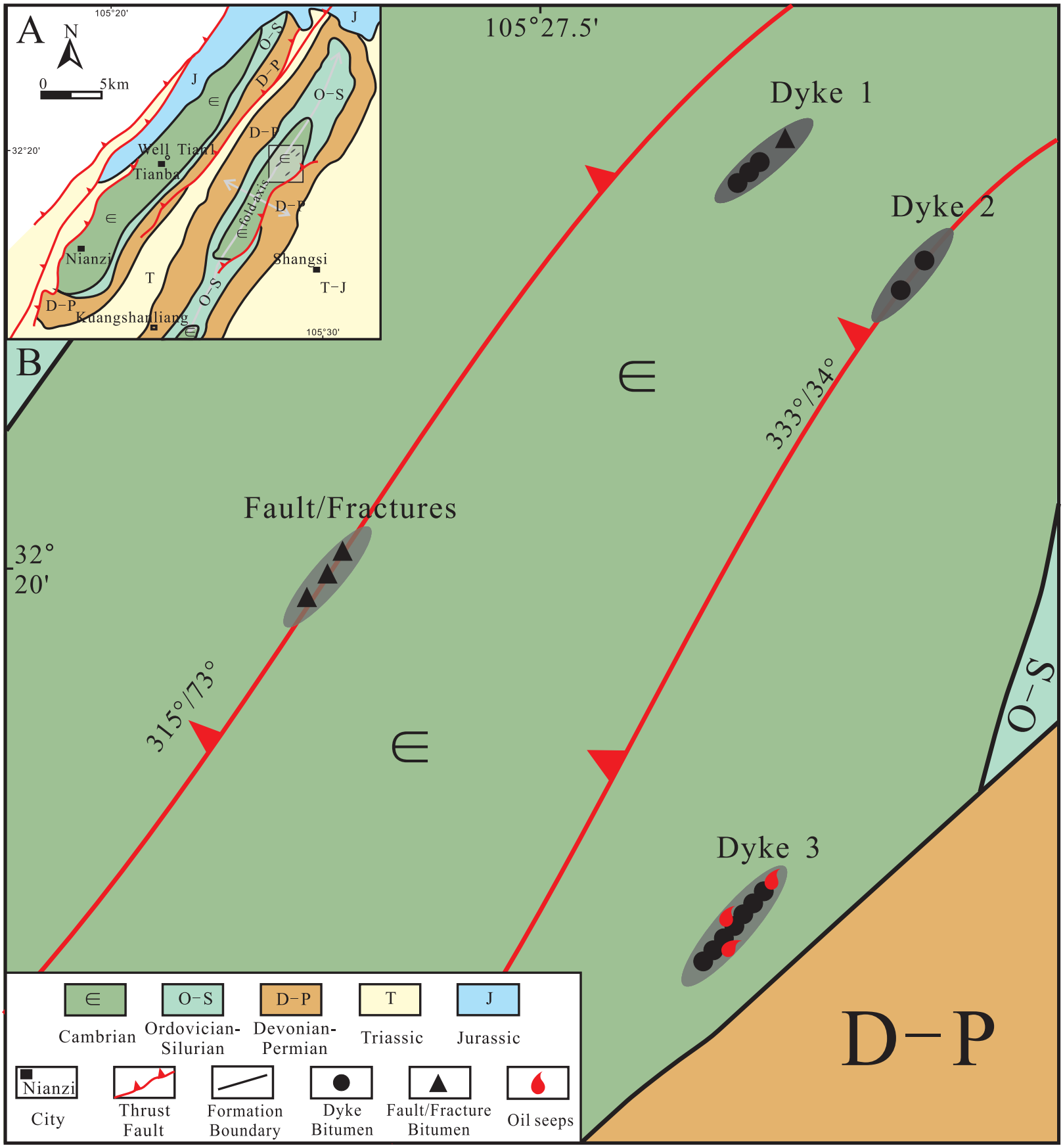

Figure 4

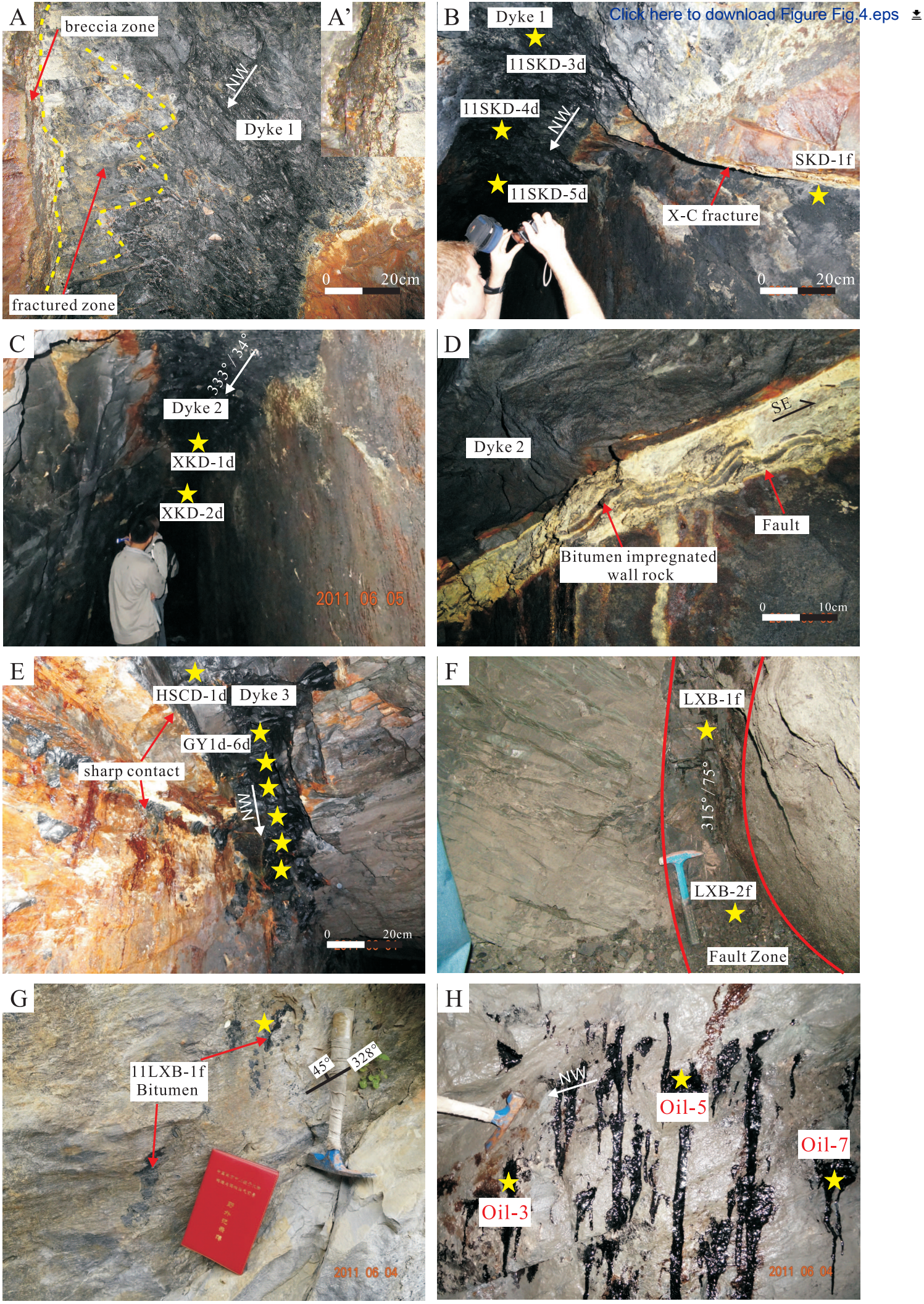

Figure 5

Click here to download Figure Fig.5.eps

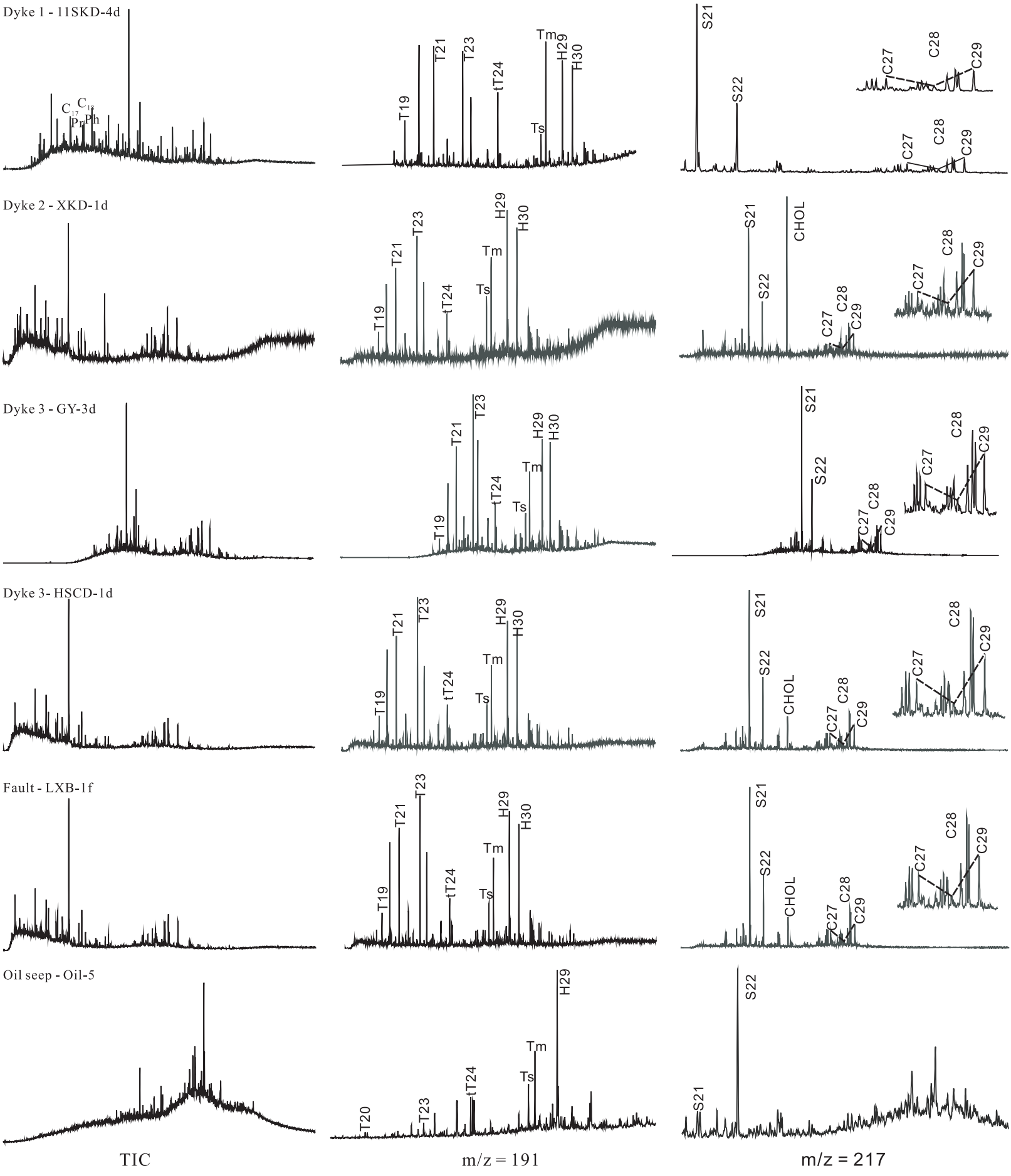

Figure 6

Click here to download Figure Fig.6.eps

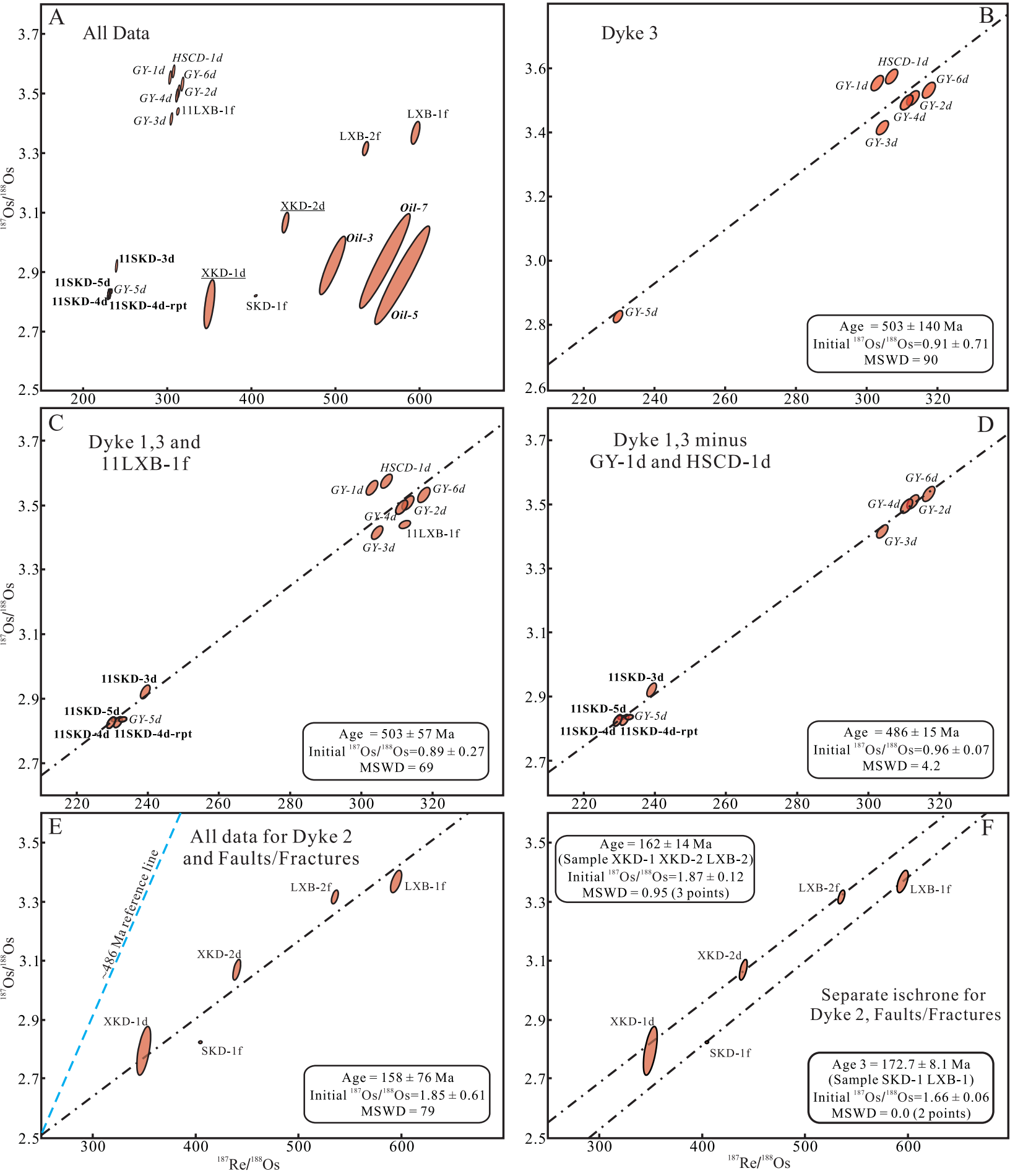

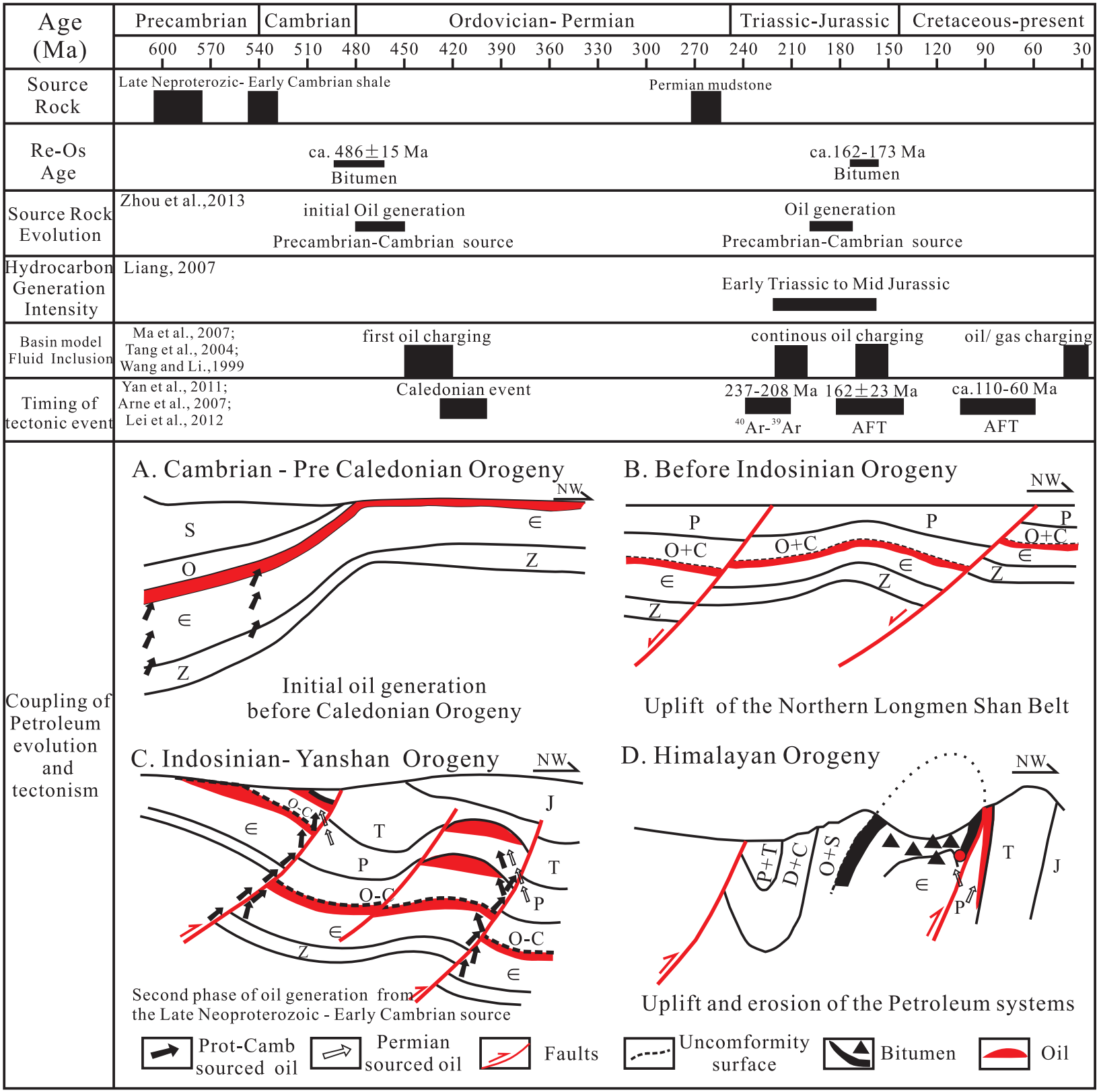

Figure 7

Table 1. The biomarker characteristics of the bitumen and present day oil seeps from the Kuangshangliang area, Northern Longmen Shan Thrust Belt

Sample name	ASPH (%)	CPI	Pr/ C17	Ph/ C18	Pr/Ph	GAM /H30	Ts/ Ts+Tm	TR23/ TR21	TR23 / tT24	tT24/ TR26	DH30 /H30	H32 S/(R+S)	NOR25H /H30	S21/ S22	C27R (%)	C28R (%)	C29R (%)	C29S /(S+R)	C29ββ/ (ββ+αα)
Dyke 1																			
11SKD-4d	/	/	0.96	1.71	0.72	0.14	0.2	0.90	1.50	2.32	0.06	0.6	0.16	2.55	34.5	19.5	46	0.5	0.49
Dyke 2																			
XKD-1d	98	1.05	0.4	1.05	0.47	0.22	0.38	1.45	2.41	1.21	0.08	0.57	0.14	2.58	24.8	15.7	59.5	0.51	0.51
Dyke 3																			
GY-1d	/	1.04	/	/	/	0.18	0.32	1.67	2.85	1.03	0.05	0.54	0.16	2.41	30.1	15.2	54.7	0.52	0.53
GY-3d	/	1.16	/	/	/	0.19	0.32	1.57	2.88	1	0.05	0.56	0.16	2.42	27.7	14.4	57.9	0.5	0.53
GY-5d	/	0.91	/	/	/	0.13	0.31	1.31	2.20	1.43	0.05	0.58	0.17	2.5	30.4	16.2	53.4	0.52	0.55
HSCD-1d	99	2.59	0.7	0.91	0.95	0.15	0.35	1.49	3.01	1.06	0.05	0.62	0.13	2.45	32.2	16.3	51.5	0.47	0.57
Fault and fractures																			
SKD-1f	98	0.94	/	/	/	0.12	0.24	1.00	1.28	2.61	0.02	0.6	0.07	2.46	29	15.2	55.7	0.46	0.5
11LXB-1	99	1.21	/	/	/	0.17	0.32	1.38	2.82	1.01	0.05	0.6	0.17	2.26	30.8	16	53.2	0.47	0.55
LXB-1f	98	0.35	/	/	/	0.18	0.33	1.38	2.83	1.00	0.06	0.58	0.19	2.32	31.90	14.80	53.40	0.46	0.55
Oil																			
Oil-3	13.54	/	/	/	/	7.59	0.37	/	/	0.51	5.54	/	/	0.21	/	/	/	/	/
Oil-5	9.48	/	/	/	/	3.91	0.36	/	0.26	0.52	3.1	/	/	0.2	/	/	/	/	/

Table 2. Re-Os elemental and isotopic data of the bitumen and present day oil seeps from the Kuangshanliang area, Northern Longmen Shan Thrust Belt.

Sample	latitude	longitude	Re (ppb)	Re blk %	Os (ppt)	Os blk %	$^{187}Re/^{188}Os$	$^{187}Os/^{188}Os$	rho	Osi_{503}	Osi_{486}	Osi_{483}	Osi_{158}
Dyke 1													
11SKD-3d	32°20'27"	105°27'47"	403.5(1.0)	0.004	11094.0(64.7)	0.007	239.1(1.1)	2.92(0.02)	0.560	/	/	0.99	/
11SKD-4d	32°20'25"	105°27'48"	512.2(1.8)	0.003	14478.3(46.3)	0.006	230.7(0.9)	2.84(0.01)	0.260	/	/	0.97	/
11SKD-4d-rpt	32°20'25"	105°27'48"	518.8(1.3)	0.010	14605.3(75.8)	0.046	231.5(1.0)	2.83(0.01)	0.567	/	/	0.96	/
11SKD-5d	32°20'26"	105°27'47"	547.9(1.9)	0.009	15347.3(50.3)	0.042	232.8(0.9)	2.84(0.01)	0.238	/	/	0.96	/
Dyke 2													
XKD-1d	32°20'26"	105°27'49"	332.9(1.1)	0.007	6182.4(80.9)	0.107	349.7(5.2)	2.79(0.07)	0.591	/	-0.05	/	1.87
XKD-2d	32°20'25"	105°27'49"	334(1.2)	0.007	5058.7(38.4)	0.133	440.2(3.2)	3.07(0.03)	0.576	/	-0.51	/	1.91
Dyke 3													
GY-1d	32°19'21"	105°27'47"	305.6(0.8)	0.008	7033.5(40.5)	0.012	302.9(1.3)	3.56(0.02)	0.581	1.01	/	1.11	/
GY-2d	32°19'20"	105°27'45"	320.3(0.8)	0.007	7105.0(40.4)	0.012	313.1(1.4)	3.51(0.02)	0.582	0.87	/	0.98	/
GY-3d	32°19'22"	105°27'47"	303.7(0.8)	0.008	6869.0(38.1)	0.012	304.4(1.3)	3.42(0.02)	0.577	0.85	/	0.96	/
GY-4d	32°19'21"	105°27'46"	293.5(0.7)	0.008	6538.1(37.2)	0.013	311.3(1.4)	3.49(0.02)	0.577	0.88	/	0.98	/
GY-5d	32°19'22"	105°27'47"	524.8(1.3)	0.005	14895.1(79.1)	0.005	229.5(1.0)	2.83(0.01)	0.562	0.89	/	0.97	/
GY-6d	32°19'20"	105°27'48"	329.3(0.8)	0.007	7216.8(42.4)	0.012	317.6(1.4)	3.53(0.02)	0.567	0.86	/	0.97	/
HSCD-1d	32°19'21"	105°27'47"	284.1(0.7)	0.006	6464.5(36.3)	0.013	307.0(1.3)	3.58(0.02)	0.581	0.99	/	1.10	/
Fault and Fracture													
11LXB-1f	32°20'07"	105°27'20"	311.1(1.1)	0.005	6875.7(29.5)	0.013	312.2(1.3)	3.44(0.01)	0.408	/	/	/	/
SKD-1f	32°20'26"	105°27'47"	525.9(1.8)	0.004	8460.4(20.0)	0.074	404.8(1.4)	2.82(<0.01)	0.468	/	-0.47	/	1.75
LXB-1f	32°20'06"	105°27'19"	352.2(1.2)	0.005	4058.2(31.6)	0.413	595.1(4.2)	3.37(0.03)	0.582	/	-1.47	/	1.80
LXB-2f	32°20'06"	105°27'20"	334.4(1.1)	0.007	4259.3(25.6)	0.409	535.6(2.8)	3.32(0.02)	0.505	/	-1.04	/	1.90
Oil													
Oil-3	32°19'20"	105°27'48"	9.6(0.1)	0.185	127.2(1.9)	3.803	496.3(12.6)	2.92(0.08)	0.88	/	/	/	/
Oil-5	32°19'21"	105°27'47"	8.1(0.1)	0.312	91.7(2.0)	3.632	579.3(26.6)	2.89(0.14)	0.948	/	/	/	/
Oil-7	32°19'20"	105°27'46"	7.7(0.1)	0.308	90.3(1.9)	3.460	558.6(24.5)	2.94(0.13)	0.947	/	/	/	/

Note: asphaltene fraction of the oil were fisrt precipitated using 40 times volume of *n*-heptane (~1 g oil with 40 ml solvent) at room temperature for at least 8 hrs and Re-Os analyses are conduct on the asphaltenes.

Dataset

Click here to access/download

Dataset

appendix Re-Os data table 20170227.xlsx

Transfer of Copyright Agreement

Copyright including rights in transmissions is hereby transferred to The American Association of Petroleum Geologists (for government employees: to the extent transferable), effective if and when the work is accepted for publication. A "transmission" for purposes of this agreement is defined as a reproduction distributed by any device or process whereby a copy of the work is fixed beyond the place from which it was sent.

Copyright to: *AAPG Bulletin (The American Association of Petroleum Geologists)*

Name of Authors: *Xiang Ge, Chuanbo Shen, David Selby, Jie Wang, Liangbang Ma, Xiaoyan Ruan, Shouzhi Hu, Lianfu Mei*

DOI:

To be signed by an author (who agrees to inform the others, if any) or, in the case of a "work made for hire," by the employer.

Signature	Chuanbo Shen Printed Name
Title (if not author)	China University of Geosciences(Wuhan) Company or Institution
2/22/2017 Date	Issue: Volume/Number (Month, Year)

P.O. Box 979, Tulsa, Okla., 74101-0979 USA • 1444 South Boulder, Tulsa, Okla., 74119-0979 USA
Phone: +1.918.584.2555 • Fax: +1.918.560.2632 • E-Mail: bulletin@aapg.org
Tulsa | Bogota| Dubai | London | Singapore | Washington, D.C.